9064 *Inorg. Chem.* **2010**, *49*, 9064–9077
DOI: 10.1021/ic101765h

Inorganic Chemistry
Article

Use of Metallopeptide Based Mimics Demonstrates That the Metalloprotein Nitrile Hydratase Requires Two Oxidized Cysteinates for Catalytic Activity

Jason Shearer,* Paige E. Callan, and Justina Amie

Department of Chemistry, University of Nevada, Reno, Nevada 89557

Received August 30, 2010

Nitrile hydratases (NHases) are non-heme Fe^{III} or non-corrin Co^{III} containing metalloenzymes that possess an N_2S_3 ligand environment with nitrogen donors derived from amidates and sulfur donors derived from cysteinates. A closely related enzyme is thiocyanate hydrolase (SCNase), which possesses a nearly identical active-site coordination environment as CoNHase. These enzymes are redox inactive and perform hydrolytic reactions; SCNase hydrolyzes thiocyanate anions while NHase converts nitriles into amides. Herein an active CoNHase metallopeptide mimic, [Co^{III}NHase-m1] (NHase-m1 = AcNH-CCDLP-CGVYD-PA-COOH), that contains Co^{III} in a similar N_2S_3 coordination environment as CoNHase is reported. [Co^{III}NHase-m1] was characterized by electrospray ionization-mass spectrometry (ESI-MS), gel-permeation chromatography (GPC), Co K-edge X-ray absorption spectroscopy (Co−S: 2.21 Å; Co−N: 1.93 Å), vibrational, and optical spectroscopies. We find that [Co^{III}NHase-m1] will perform the catalytic conversion of acrylonitrile into acrylamide with up to 58 turnovers observed after 18 h at 25 °C (pH 8.0). FTIR data used in concert with calculated vibrational data (mPWPW91/aug-cc-TZVPP) demonstrates that the active form of [Co^{III}NHase-m1] has a ligated SO_2 (ν = 1091 cm^{-1}) moiety and a ligated protonated SO(H) (ν = 928 cm^{-1}) moiety; when only one oxygenated cysteinate ligand (i.e., a mono-SO_2 coordination motif) or the bis-SO_2 coordination motif are found within [Co^{III}NHase-m1] no catalytic activity is observed. Calculations of the thermodynamics of ligand exchange (B3LYP/aug-cc-TZVPP) suggest that the reason for this is that the SO_2/SO(H) equatorial ligand motif promotes both water dissociation from the Co^{III}-center and nitrile coordination to the Co^{III}-center. In contrast, the under- or overoxidized motifs will either strongly favor a five coordinate Co^{III}-center or strongly favor water binding to the Co^{III}-center over nitrile binding.

Introduction

Nitrile hydratases (NHases) are an industrially important class of redox-inactive non-heme Fe^{III} or non-corrin Co^{III} metalloenzymes that effect the conversion of nitriles into amides (Figure 1a).[1−6] A structurally related class of metalloenzymes are thiocyanate hydrolases (SCNases), which convert the SCN^- anion into NH_3 and SCO (Figure 1b).[7−9] X-ray crystal structures are available for both the cobalt (CoNHase) and the iron forms (FeNHase) of NHase as well as SCNase, whose active-site structure is nearly identical to that of CoNHase.[8−15] In all three metalloenzymes the M^{III} ion is ligated by three cysteinate sulfurs in a *fac* configuration and two amidate nitrogen ligands derived from the protein backbone. One of the cysteinate sulfurs is *trans* to a site that has been speculated to be occupied by a water (or hydroxide) molecule (or NO in the FeNHase inactivated form), but could also be a vacant site in the absence of substrate.[10,11,13] An interesting structural aspect of the NHase and SCNase active site concerns the two cysteinate sulfurs that are contained within the metal-center's equatorial plane; crystallographic

*To whom correspondence should be addressed. E-mail: shearer@unr.edu.

(1) Kovacs, J. A. *Chem. Rev.* **2003**, *104*, 823–848.
(2) De Santis, G.; Di Cosimo, R. *Biocatal. Pharm. Ind.* **2009**, 153–181.
(3) Kobayashi, M.; Shimizu, S. *Eur. J. Biochem.* **1999**, *261*, 1–9.
(4) Wieser, M.; Nagasawa, T. *Stereosel. Biocatal.* **2000**, 461–486.
(5) Harrop, T. C.; Mascharak, P. K. *Acc. Chem. Res.* **2004**, *37*, 253–260.
(6) Nagasawa, T.; Takeuchi, K.; Yamada, H. *Eur. J. Biochem.* **1991**, *196*, 581–589.
(7) Katayama, Y.; Nyunoya, H. *Baiosaiensu to Indasutori* **1999**, *57*, 387–390.
(8) Arakawa, T.; Kawano, Y.; Kataoka, S.; Katayama, Y.; Kamiya, N.; Yohda, M.; Odaka, M. *J. Mol. Biol.* **2007**, *366*, 1497–1509.
(9) Katayama, Y.; Hashimoto, K.; Nakayama, H.; Mino, H.; Nojiri, M.; Ono, T.-A.; Nyunoya, H.; Yohda, M.; Takio, K.; Odaka, M. *J. Am. Chem. Soc.* **2006**, *128*, 728–729.
(10) Arakawa, T.; Kawano, Y.; Katayama, Y.; Nakayama, H.; Dohmae, N.; Yohda, M.; Odaka, M. *J. Am. Chem. Soc.* **2009**, *131*, 14838–14843.
(11) Huang, W.; Jia, J.; Cummings, J.; Nelson, M.; Schneider, G.; Lindqvist, Y. *Structure* **1997**, *5*, 691–699.
(12) Miyanaga, A.; Fushinobu, S.; Ito, K.; Wakagi, T. *Biochem. Biophys. Res. Commun.* **2001**, *288*, 1169–1174.
(13) Nagashima, S.; Nakasako, M.; Dohmae, N.; Tsujimura, M.; Takio, K.; Odaka, M.; Yohda, M.; Kamiya, N.; Endo, I. *Nat. Struct. Biol.* **1998**, *5*, 347–351.
(14) Nakasako, M.; Odaka, M.; Yohda, M.; Dohmae, N.; Takio, K.; Kamiya, N.; Endo, I. *Biochemistry* **1999**, *38*, 9887–9898.
(15) Song, L.; Wang, M.; Shi, J.; Xue, Z.; Wang, M.-X.; Qian, S. *Biochem. Biophys. Res. Commun.* **2007**, *362*, 319–324.

Published on Web 09/10/2010

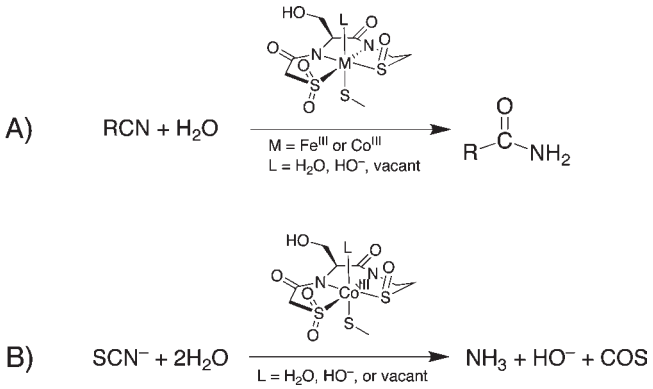

Figure 1. (A) Reaction catalyzed by nitrile hydratases and (B) reaction catalyzed by thiocyanate hydrolase. Note the similarity in purported active-site structures.

analysis has suggested that these are post-translationally oxygenated to the corresponding sulfenate/sulfenic acid ($CysSO^-$/CysSO(H)) and a sulfinate ($Cys-SO_2$). To our knowledge these two classes of metalloenzymes represent the only metalloenzymes containing this oxidized cysteinate coordination motif.

Several X-ray structures have been reported for both NHase and SCNase with varying degrees of equatorial cysteinate oxygenation.[8−15] From these studies it has been suggested that insertion of the M^{III} ion into the active-site and formation of the sulfinate proceeds nearly simultaneously. Sulfenate formation, at least in recombinant SCNase, appears to occurs at a later time.[10] In addition to X-ray crystallographic studies, the formulation of the post-translationally modified cysteinates as one sulfenate and one sulfinate ligated to the M^{III} ion has also been supported by spectroscopic (sulfur K-edge X-ray absorption spectroscopy and FTIR spectroscopy)[16,17] and mass spectrometry studies.[18−21] We note that the sulfur K-edge X-ray absorption and FTIR spectroscopic studies have suggested that the sulfenate is likely protonated or contained in a strong hydrogen-bonding network.[16,17]

Mass spectrometry studies have provided fairly convincing evidence that *at least* one of the cysteinates must be post-translationally modified to a $CysSO_2$ ligand for NHases to display activity; combined liquid chromatography-mass spectrometry (LC-MS)/activity studies have directly correlated enzymatic activity with cysteinate oxygenation.[18] Furthermore, when FeNHase is prepared under anaerobic conditions, where cysteinate oxidation would be unlikely, no enzymatic activity is observed.[18] Upon exposure of anaerobically prepared FeNHase to air, the enzyme becomes activated. In fact, most industrial processes that utilize NHase involve maintaining the enzyme under constant aerobic or oxidizing conditions to maintain optimal NHase activity.[22−25] There has also been one combined X-ray crystallography/activity study involving SCNase that has produced some evidence that the sulfinate/sulfenate modification is necessary for full enzymatic activity; modification of only one cysteinate to the sulfinate and the bis-sulfinate modification each produces lowered enzymatic activity.[10] For NHase it is not so clear-cut, with studies suggesting that overoxidation can either lead to enzymatic deactivation *or* produce a fully active metalloenzyme.[15,26] When 2-cyano-2-propyl hydroperoxide (CPx) is added to active FeNHase it will strongly inhibit the metalloenzyme. As CPx is capable of oxidizing sulfenates to sulfinates it was suggested that the loss of activity is likely due to the oxidation of the CysSO ligand to a $CysSO_2$ ligand.[26] However, CPx is also capable of reacting with the Fe^{III} metal-center generating an Fe^{II} ion in the process. This metal-based reduction event would also lead to enzymatic deactivation. LC-MS studies also *indirectly* provide evidence of a sulfenate in the active form of NHase. All of the mass spectrometry studies that can identify the "Cys-SO" ligand in the active form of NHase rely on a trypsin digestion of the metalloenzyme. In these studies the Cys-SO is never observed by MS in the sulfenate form, but in the sulfinate form.[18−21] There are three possible explanations for this observation. One is that the inherently reactive Cys-SO moiety readily oxidizes to the corresponding Cys-SO_2 group under the experimental conditions used to detect it (i.e., trypsin digestion followed by MS/MS analysis). Another possibility is that the cysteinate remains completely *unmodified* in the active form of NHase and that the oxidation of the unmodified equatorial Cys to the Cys-SO(H) or $CysSO_2$ form results in enzymatic inactivity. The oxidized cysteinate observed by ESI-MS may therefore be an artifact of the experiment. A third possibility is that the fully oxidized bis-$CysSO_2$ form of NHase is required for activity, and that the supposition that the *underoxidized* sulfenate is present at the active-site of the active form of NHase is incorrect. This third possibility is supported by limited structural/mechanistic considerations resulting from a recent crystallographic study of CoNHase.[15]

Much of the ambiguity concerning the requirement of one versus two oxygenated cysteinates coordinated to the M^{III} ion at the NHase and SCNase active-sites and the exact extent of cysteinate oxygenation stems from the lack of studies that are capable of directly correlating enzymatic activity with the extent of cysteinate oxygenation. From a biochemical perspective this is exceptionally difficult because of the inherent lack of fidelity with concern to cysteinate-oxygenation. This is exacerbated by the difficulty of directly monitoring cysteinate-oxygenation as a function of enzymatic activity because the available techniques for doing so

(16) Dey, A.; Chow, M.; Taniguchi, K.; Lugo-Mas, P.; Davin, S.; Maeda, M.; Kovacs, J. A.; Odaka, M.; Hodgson, K. O.; Hedman, B.; Solomon, E. I. *J. Am. Chem. Soc.* **2006**, *128*, 533–541.
(17) Noguchi, T.; Nojiri, M.; Takei, K.-i.; Odaka, M.; Kamiya, N. *Biochemistry* **2003**, *42*, 11642–11650.
(18) Murakami, T.; Nojiri, M.; Nakayama, H.; Odaka, M.; Yohda, M.; Dohmae, N.; Takio, K.; Nagamune, T.; Endo, I. *Protein Sci.* **2000**, *9*, 1024–1030.
(19) Claiborne, A.; Mallett, T. C.; Yeh, J. I.; Luba, J.; Parsonage, D. *Adv. Protein Chem.* **2001**, *58*, 215–276.
(20) Nojiri, M.; Yohda, M.; Odaka, M.; Matsushita, Y.; Tsujimura, M.; Yoshida, T.; Dohmae, N.; Takio, K.; Endo, I. *J. Biochem.* **1999**, *125*, 696–704.
(21) Stevens, J. M.; Belghazi, M.; Jaouen, M.; Bonnet, D.; Schmitter, J.-M.; Mansuy, D.; Sari, M.-A.; Artaud, I. *J. Mass Spectrom.* **2003**, *38*, 955–961.
(22) Ito, K.; Yakami, T.; Arii, T.; Tsuruoka, M.; Nakamura, T. (Mitsui Toatsu Chemicals, Incorporated, Japan); European Patent Application 790310, 1997, p 84.
(23) Tamura, K. (Nitto Chemical Industry Co., Ltd., Japan); European Patent Application 711836, 1996, p 10.
(24) Yamada, H.; Nagasawa, T. (Nitto Kagaku Kogyo K. K., Japan; Nitto Chemical Industry Co., Ltd.); European Patent Application 362829, 1990, p 9.
(25) Yamaguchi, Y.; Ushigome, M.; Kato, T. (Nitto Chemical Industry Co., Ltd., Japan; Mitsubishi Rayon Co., Ltd.); European Patent Application 773297, 1997, p 11.
(26) Tsujimura, M.; Odaka, M.; Nakayama, H.; Dohmae, N.; Koshino, H.; Asami, T.; Hoshino, M.; Takio, K.; Yoshida, S.; Maeda, M.; Endo, I. *J. Am. Chem. Soc.* **2003**, *125*, 11532–11538.

Chart 1

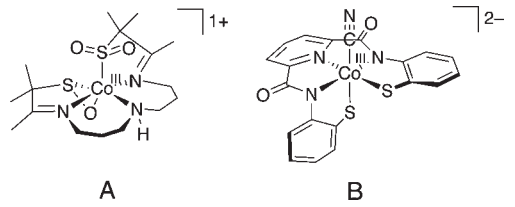

A B

offer either nearly insurmountable signal-to-noise/overlapping signal problems (e.g., protein FTIR) or the introduction of additional artifacts (e.g., trypsin digestions).

Biomimetic NHase complexes have proven useful in understanding many of the key structural components of the NHase active-site, and how these components contribute to the electronic structure and bonding properties of the metalloenzyme.[1,5,27−29] To date several NHase mimics have been prepared that contain oxygenated thiolate ligands.[30−41] Most of these complexes contain bis-sulfinate ligands; only one model compound has been reported thus far that contains both a sulfenate and a sulfinate coordinated to the metal-ion (a CoNHase model reported by Kovacs and co-workers; Chart 1a).[33] Although this compound revealed a number of interesting aspects of CoNHase chemistry, including the likely order of addition of oxygen atoms to the coordinated thiolate-sulfurs, the sulfenate oxygen of this compound is coordinated to the Co^{III} center, and the compound does not display NHase activity. Likewise, only one NHase model compound (a CoNHase model complex reported by Mascharak and co-workers; Chart 1b) has been reported thus far that displays any NHase activity.[42] This model complex, although active (18 turnovers after 4 h), contains *no* oxygenated thiolates, and is reactive at relatively high temperatures (50 °C) and pH (9.5). An initial report on the oxidation of the thiolate *trans* to the open site of Mascharak's model suggested an enhancement in catalytic activity.[38] To better correlate activity with thiolate-oxidation one needs a compound that (a) can under go sequential thiolate oxygenation and (b) displays at least modest NHase activity.

Reported herein is a metallopeptide CoNHase mimic that displays reasonable catalytic activity under optimal conditions (approximately 60 turnovers in 18 h at 25 °C). Furthermore, through controlling the extent of cysteinate oxygenation, we can directly correlate the extent of oxygenation with catalytic activity. It will be demonstrated that catalytic activity requires oxygenation of two cysteinate, one to a Cys-SO_2 and the other to a protonated Cys-SO(H).

Experimental Section

Preparation of NHase-m1. The apo-peptide NHase-m1 (AcNH-CCDLP-CGVYD-PA-COOH) was prepared in a manner similar to that previously reported for similar peptides using solid-state peptide synthesis methods (Fmoc/tBu protection strategies) on Wang resin.[43−46] The peptide was cleaved from the resin using a 95:2.5:2.5 mixture of trifluoroacetic acid(TFA)/triisopropylsilane/ethanedithiol. Following evaporation of the cleavage solution, the resulting crude peptide was washed with freshly distilled diethyl ether and purified by reverse-phase HPLC (gradient: 10−29% MeCN (0.1% TFA) in H_2O (0.1% TFA) over 15 min) using a Waters DeltaPrep 600 equipped with a Waters X-Bridge C-18 column (30 × 150 mm; 5 μm). Fractions containing NHase-m1 were pooled and lyophilized yielding a white fluffy solid (26.3 mg; Yield =20.3%). Final purity was assessed by analytical HPLC using a Waters X-Bridge C-18 column (4.6 × 150 mm; 5 μm) on a Waters DeltaPrep 60 and ESI-MS on a Waters MicroMass 20 ESI mass spectrometer (positive ion mode). (Analytical HPLC−gradient: 10−65% MeCN (0.1% TFA) in H_2O (0.1% TFA) over 60 min; Retention time: 20.7 min. ESI-MS (pos. ion mode) - $(M+Na)^+$ m/z calcd 1319.4; found 1320.0).

Metalation and Maturation of NHase-m1 with Cobalt. NHase-m1 was dissolved in degassed 10 mM *N*-ethylmorpholine buffer (NEM; pH 8.0) under an inert atmosphere yielding a final concentration of approximately 1.0 mM as assessed by the absorbance of the charge transfer band associated with the Y(9) residue (λ_{max}= 278 nm; ε = 1,490 M^{-1} cm^{-1}).[47] Using Ellmans' methods, we verified that all of the cysteine residues were free, and no further treatment of the peptide solution was performed.[48] The addition of 1 equiv of $CoCl_2$ under strictly anaerobic conditions in a Coy chamber resulted in the immediate formation of a light colored green solution (λ_{max}= 736 nm; ε = 425 M^{-1} cm^{-1}; λ_{max}= 687 nm; ε = 510 M^{-1} cm^{-1}; λ_{max}= 611 nm; ε = 405 M^{-1} cm^{-1}; and λ_{max}= 340 nm; ε = 2113 M^{-1} cm^{-1}) indicating the formation of [Co^{II}NHase-m1]. Exposure to air resulted in the conversion of the green solution into a brown one within 10 min. After 3 h the solution became a deep brown, by which time the fully functional metallopeptide [Co^{III}NHase-m1] had formed. The solution was then purged with argon and could be stored indefinitely under an inert atmosphere. Subsequent gel-permeation chromatography (GPC) experiments were performed using a Waters Protein-Pak GPC column (7.8 × 300 mm; 60 Å pore size) using a $NaHCO_3$(aq.) mobile phase under a positive pressure of He. GPC calibrations were made using a Water polyethyleneglycol standards kit. (Mass by GPC: calc. 1398 g mol^{-1} found 1395 g mol^{-1}; ESI-MS (negative ion mode) m/z calc. 1398.4 found 1398;

(27) Mascharak, P. K. *Coord. Chem. Rev*. **2002**, *225*, 201–214.
(28) O'Toole, M. G.; Grapperhaus, C. A. *ACS Symp. Ser*. **2009**, *1012*, 99–113.
(29) Artaud, I.; Chatel, S.; Chauvin, A. S.; Bonnet, D.; Kopf, M. A.; Leduc, P. *Coord. Chem. Rev*. **1999**, *190−192*, 557–586.
(30) Bourles, E.; Alves de Sousa, R.; Galardon, E.; Giorgi, M.; Artaud, I. *Angew. Chem., Int. Ed*. **2005**, *44*, 6162–6165.
(31) Galardon, E.; Giorgi, M.; Artaud, I. *Chem. Commun*. **2004**, 286–287.
(32) Rat, M.; Alves de Sousa, R.; Vaissermann, J.; Leduc, P.; Mansuy, D.; Artaud, I. *J. Inorg. Biochem*. **2001**, *84*, 207–213.
(33) Kung, I.; Schweitzer, D.; Shearer, J.; Taylor, W. D.; Jackson, H. L.; Lovell, S.; Kovacs, J. A. *J. Am. Chem. Soc*. **2000**, *122*, 8299–8300.
(34) Lugo-Mas, P.; Dey, A.; Xu, L.; Davin, S. D.; Benedict, J.; Kaminsky, W.; Hodgson, K. O.; Hedman, B.; Solomon, E. I.; Kovacs, J. A. *J. Am. Chem. Soc*. **2006**, *128*, 11211–11221.
(35) Lugo-Mas, P.; Taylor, W.; Schweitzer, D.; Theisen, R. M.; Xu, L.; Shearer, J.; Swartz, R. D.; Gleaves, M. C.; DiPasquale, A.; Kaminsky, W.; Kovacs, J. A. *Inorg. Chem*. **2008**, *47*, 11228–11236.
(36) Rose, M. J.; Betterley, N. M.; Mascharak, P. K. *J. Am. Chem. Soc*. **2009**, *131*, 8340–8341.
(37) Rose, M. J.; Betterley, N. M.; Oliver, A. G.; Mascharak, P. K. *Inorg. Chem*. **2010**, *49*, 1854–1864.
(38) Tyler, L. A.; Noveron, J. C.; Olmstead, M. M.; Mascharak, P. K. *Inorg. Chem*. **2003**, *42*, 5751–5761.
(39) O'Toole, M. G.; Kreso, M.; Kozlowski, P. M.; Mashuta, M. S.; Grapperhaus, C. A. *J. Biol. Inorg. Chem*. **2008**, *13*, 1219–1230.
(40) Yano, T.; Arii, H.; Yamaguchi, S.; Funahashi, Y.; Jitsukawa, K.; Ozawa, T.; Masuda, H. *Eur. J. Inorg. Chem*. **2006**, 3753–3761.
(41) Yano, T.; Wasada-Tsutsui, Y.; Arii, H.; Yamaguchi, S.; Funahashi, Y.; Ozawa, T.; Masuda, H. *Inorg. Chem*. **2007**, *46*, 10345–10353.
(42) Noveron, J. C.; Olmstead, M. M.; Mascharak, P. K. *J. Am. Chem. Soc*. **1999**, *121*, 3553–3554.
(43) Shearer, J.; Long, L. M. *Inorg. Chem*. **2006**, *45*, 2358–2360.
(44) Neupane, K. P.; Shearer, J. *Inorg. Chem*. **2006**, *45*, 10552–10566.
(45) Neupane, K. P.; Gearty, K.; Francis, A.; Shearer, J. *J. Am. Chem. Soc*. **2007**, *129*, 14605–14618.
(46) Shearer, J.; Neupane, K. P.; Callan, P. E. *Inorg. Chem*. **2009**, *48*, 10560–10571.
(47) Du, H.; Fuh, R. A.; Li, J.; Corkan, A.; Lindsey, J. S. *Photochem. Photobiol*. **1998**, *68*, 141–142.
(48) Ellman, G. L. *Arch. Biochem. Biophys*. **1958**, *74*, 443–450.

λ_{max} = 453 nm (sh); ε = 1350 M^{-1} cm^{-1}; λ_{max} = 332 nm (sh); ε = 3255 M^{-1} cm^{-1})

Physical Methods. Electronic absorption spectra were obtained in airtight quartz cuvettes using either a Varian CARY 50 or a Perkin-Elmer Lambda 750 UV−vis−NIR spectrometer. Circular dichroism spectra were obtained on a Jasco J-715 CD spectropolarimeter in circular 1 cm quartz cuvettes and represent the average of five scans. Electronic absorption and CD spectra were simultaneously deconvoluted into the minimum number of Gaussian line shapes that reproduced the two spectra using in-house written procedures for the data analysis and graphing program Igor Pro (Wavemetrics; Lake Oswego, OR). We used the criteria that all peak widths were within ±500 cm^{-1} of 11 × $(\nu)^{0.5}$ to ensure a meaningful fit to the absorption spectrum.

FTIR spectra were obtained on a Thermo-Nicolet 470 FTIR spectrometer with either a SMART MIRacle Attenuated Total Reflectance (ATR) accessory (as dehydrated films formed from the addition of 10 μL of sample to the ZnSe crystal) or in a liquid sample holder between CaF_2 plates. Approximately 1 mM solutions of [Co^{III}NHase-m1] in 10 mM NEM (pH 8.0) were used in all experiments. A background of a 1 mM solution of the apo-peptide NHase-m1 in 10 mM NEM buffer (pH 8.0) was used for all experiments. For time course experiments, solutions of [Co^{II}NHase-m1] were exposed to air, and then the FTIR spectra were obtained after specified time intervals. In all cases the spectra represent the average of 1000 scans at 1 cm^{-1} resolution except for the spectra following 10 min of air exposure, which represents the average of only 160 scans at 1 cm^{-1} resolution. Data were then normalized to a positive-signed peak in the difference spectrum at 1261 cm^{-1}, which is invariant in relative intensity between spectra. $^{18}O_2$ labeling was performed by injecting 98% enriched $^{18}O_2$ gas (ICON Isotopes; Summit, NJ) via an airtight syringe into a solution of [Co^{II}NHase-m1]. The IR spectrum of the $^{18}O_2$ matured metallopeptide was then recorded after 3 h of maturation (1000 scans at 1 cm^{-1} resolution). H/D exchange studies were performed using [Co^{III}NHase-m1] that was matured in D_2O buffer (10 mM NEM, pD = 8.0).

Cobalt K-edge X-ray absorption spectra were obtained at the National Synchrotron Light Source on beamline X3b. Samples of O_2 matured [Co^{III}NHase-m1] in a 1:1 mixture of 10 mM NEM buffer (pH 8.0) and glycerol were injected between windows made from Kapton tape (3M; Minneapolis, MN, catalog no. 1205) and quickly frozen in liquid nitrogen. Data were collected at 20 K maintained by a He Displex cryostat and recorded as fluorescence spectra on a Canberra 13-element solid-state Ge detector. Total count rates were maintained under 25 kHz for all channels, and a dead time correction was not applied. For edge spectra the primary hutch aperture height (PHAH) was set to 0.4 mm to obtain the maximum spectral resolution in the edge region, while for the EXAFS spectra the PHAH was set to 0.8 mm. The edge spectra data were then collected in 5 eV steps in the pre-edge region (7609−7689 eV), 0.3 eV steps in the edge region (7689−7729 eV), and 2.0 eV steps in the near-edge region (7729−7909 eV). EXAFS spectra were recorded in 10 eV steps in the pre-edge region (7509−7689 eV), 0.5 eV steps in the edge region (7689−7759 eV), and 2.0 eV steps in the near-edge region (7759−8009 eV), and 5 eV steps in the far-edge region (8009−15.5 k). The spectra represents the average of 5 scans. Prior to data averaging each detector channel of each spectrum was individually inspected. Data were analyzed using the software packages EXAFS123[49] and FEFF 8.20[50] as previously described.[44] All refinements are based on Fourier Filtered $k^3(\chi)$ data over the energy range of k = 2.0−14.3 Å and back-transformed from r' = 1.0−2.5 Å. A bond valence sum (BVS) analysis was then performed on the various statistically valid models obtained form the EXAFS data.[51] The BVS is the sum of the individual bond valences (s_i) defined by

$$s_i = \exp\left[\frac{r_i - r_o}{0.37}\right] \quad (1)$$

$$\mathrm{BVS} = \sum_i s_i \quad (2)$$

where r_i are the refined bond length from the EXAFS experiments and r_o are the reference bond lengths. Here we use the method described by Brown and Altermatt for determining the values of r_o for the various Co−L bonds, and use the following values: Co−S, 2.079 Å; Co−N, 1.759 Å; Co−O, 1.687 Å.[51]

Nitrile Hydrolysis Studies. All aqueous solutions were prepared from water that had been passed through a three filter purifier to a final resistance of at least 18 MΩ. Nitrile hydrolysis was assessed by ^{13}C NMR spectroscopy and GC-mass spectrometry. In a typical experiment a 0.10 mM solution of [Co^{III}NHase-m1] in 10 mM NEM buffer (pH 8.0) was added to a 10 mM nitrile solution in pure water (total volume 300 μL). The reaction mixture was then heated to 50 °C, except for acrylonitrile hydrolysis experiments where the solution was only heated to 25 °C to avoid unwanted polymerization of the nitrile substrate. Following 18 h the reaction mixtures were analyzed. GC/MS analysis was performed by creating standard curves of nitrile and amide peak areas versus the peak area of a known quantity of *n*-octane standard. For ^{13}C NMR analysis 300 μL of D_2O (with a DDS standard) was added, and the integrated peak areas of the quaternary carbon atoms were measured and compared to a standard curve.

Electronic Structure Calculations. All density functional theory (DFT) calculations were performed using the software package ORCA 2.6.35 written by Neese and co-workers.[52] Truncated computational models of the predicted [Co^{III}NHase-m1] coordination sphere were constructed from a AcN-Cys-Cys-H fragment about a Co^{III} ion with an additional equatorial ethanethiolate ligand. A sixth ligand (water or acetonitrile) was then added to the coordination sphere about cobalt. Models containing successive thiolate oxidation were then prepared along with sulfenate protonation. This produced 15 possible models, of which the 12 models discussed in this manuscript are outlined in Chart 2. All calculations utilized Ahlrichs' TZVPP basis set[53−55] augmented by Dunning's diffuse functions.[56−58] Initial geometry optimizations were performed using the local density approximation of Vosko, Wilk, and Perdew and the nonlocal gradient corrections of Beck and Perdew.[59−64] These were then further refined with the modified Perdew−Wang 91 exchange and Perdew−Wang 91

(49) Scarrow, R. S.; Shearer, J. *EXAFS123*, v. 0.10a; University of Nevada, Reno: Reno, NV, 2010.
(50) Ankudinov, A. L.; Ravel, B.; Rehr, J. J.; Conradson, S. D. *Phys. Rev. B: Condens. Matter Mater. Phys.* **1998**, *58*, 7565–7576.
(51) Brown, I. D.; Altermatt, D. *Acta Crystallogr., Sect. B: Struct. Sci.* **1985**, *B41*, 244–247.
(52) Neese, F. N. *ORCA: An Ab Initio, Density Functional, and Semi-emperical Program Package*, v. 2.6.35; Universitat Bonn: Bonn, Germany, 2008.
(53) Schaefer, A.; Horn, H.; Ahlrichs, R. *J. Chem. Phys.* **1992**, *97*, 2571.
(54) Weigend, F.; Häser, H.; Patzelt, H.; Ahlrichs, R. *Chem. Phys. Lett.* **1998**, *294*, 143.
(55) The Ahlrichs (2df,2pd) polarization functions were obtained from the TurboMole basis set library under ftp.chemie.unikarlsruhe.de/pub/basen.
(56) Dunning, T. H., Jr. *J. Chem. Phys.* **1989**, *90*, 1007.
(57) Woon, D. E.; Dunning, T. H., Jr. *J. Chem. Phys.* **1993**, *98*, 1358.
(58) Woon, D. E.; Dunning, T. H., Jr.; as obtained from the TurboMole basis set library under ftp.chemie.uni-karlsruhe.de/pub/basen.
(59) Vosko, S. H.; Wilk, L.; Nusair, M. *Can. J. Phys.* **1980**, *58*, 1200–1211.
(60) Becke, A. D. *J. Chem. Phys.* **1986**, *84*, 4524–4529.
(61) Becke, A. D. *J. Chem. Phys.* **1988**, *88*, 1053–1062.
(62) Becke, A. D. *Phys. Rev. A: Gen. Phys.* **1988**, *38*, 3098–3100.
(63) Perdew, J. P. *Phys. Rev. B: Condens. Matter Mater. Phys.* **1986**, *33*, 8822–8824.
(64) Perdew, J. P. *Phys. Rev. B: Condens. Matter Mater. Phys.* **1986**, *34*, 7406.

Chart 2. Computational Models Examined in This Study: (A) (Co-NHase-SO_2-L)$^{2-}$ (**2-L**), (B) (Co-NHase-SO_2/SO-L)$^{2-}$ (**3-L**), (C) (Co-NHase-SO_2/SOH-L)$^{-}$ (**4-L**), (D) (Co-NHase-2SO_2-L)$^{2-}$ (**5-L**)[a]

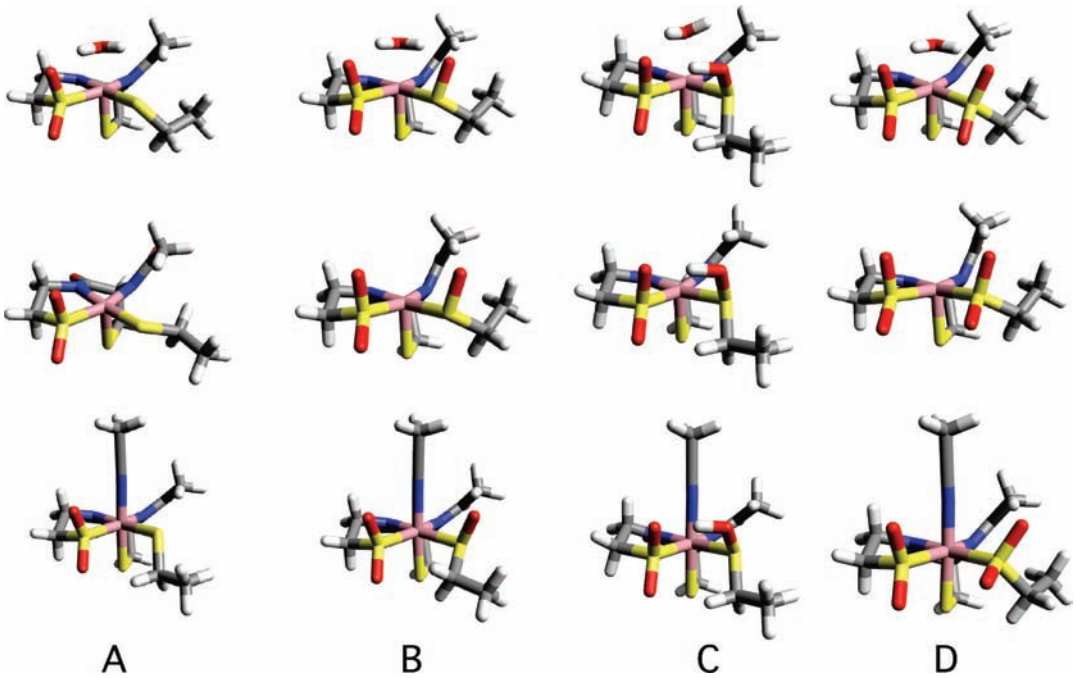

[a] In all cases L = H_2O (top), vacant (middle, abbreviated with no ligand description), or MeCN (bottom).

correlation functionals.[63,65,66] Bonding indices are described by using a Mayer bonding analysis.[67−69] All vibrational analyses utilized two sided displacements, the modified Perdew−Wang 91 exchange and Perdew−Wang 91 correlation functionals, and made use of the resolution of identity (RI) approximation[70−76] with the corresponding TZV/C auxiliary basis set.[55,77] Electronic spectra were calculated using Neese's SORCI methodology on the five lowest energy spin-allowed transitions (CAS-SCF(8,8); selection threshold = 10^{-6} E_h; prediagonalization threshold = 10^{-6} E_h; natural orbital selection threshold = 10^{-5} E_h).[78]

Calculation of Free Energies of Ligand Displacement. The free energies of relevant stationary points were calculated using Gaussian 03[79] employing the above prescribed basis sets and Becke's three-parameter hybrid functional for exchange along with the Lee−Yang−Parr correlation functional (B3LYP).[80−82] For these calculations a T = 298.15 K, a 1.0 M concentration, and a P = 1.0 atm were all utilized. All free energies are zero-point corrected. Energies were calculated from the thermodynamic scheme depicted in Scheme 1.[83] The free energies of solvation (ΔG_n) were calculated using the self-consistent reaction field model with a dielectric constant of 80.37 and probe radius of 1.4 Å.[84]

Sulfenate pK_a values were calculated according to the square-scheme displayed in Scheme 2.[83] Here we used experimental values of −262.23 kcal mol^{-1} for the free energy released upon transferring a proton from the gas-phase to water and −6.28 kcal mol^{-1} for the free energy of a proton in the gas-phase.[85,86] The pK_a was then calculated according to eq 3.

$$\mathrm{p}K_{\mathrm{a}} = \frac{1}{2.303RT}\Delta G \qquad (3)$$

Results

In previous studies we have utilized the first 12 residues from the primary sequence of nickel containing superoxide dismutase (NiSOD) from *Streptomyces coelicolor* to prepare active NiSOD biomimetic metallopeptides (apo-peptide: H_2N-HCDLP-CGVYD-PA-COOH).[43,44,46] This metallopeptide provides the nickel ion with an equatorial N_2S_2 coordination environment and an axial imidazole ligand (from His(1)) to the oxidized Ni^{III} center (Scheme 3). It was reasoned that this peptide would make an excellent platform for the production of a NHase metallopeptide-based mimic following minor modifications to the apo-peptide. Thus, the

(65) Perdew, J. P.; Chevary, J. A.; Vosko, S. H.; Jackson, K. A.; Pederson, M. R.; Singh, D. J.; Fiolhais, C. *Phys. Rev. A: Gen. Phys.* **1992**, *46*, 6671.
(66) Adamo, C.; Barone, V. *J. Chem. Phys.* **1998**, *108*, 664–675.
(67) Mayer, I. *Chem. Phys. Lett.* **1983**, *97*, 270.
(68) Mayer, I. *Int. J. Quantum Chem.* **1984**, *26*, 151.
(69) Mayer, I. *Theor. Chim. Acta* **1985**, *67*, 315.
(70) Kendall, R. A.; Früchtl, H. A. *Theor. Chem. Acc.* **1997**, *97*, 158.
(71) Eichkorn, K.; Treutler, O.; Öhm, H.; Häser, M.; Ahlrichs, R. *Chem. Phys. Lett.* **1995**, *240*, 283.
(72) Eichkorn, K.; Weigend, F.; Treutler, O.; Ahlrichs, R. *Theor. Chem. Acc.* **1997**, *97*, 119.
(73) Whitten, J. L. *J. Chem. Phys.* **1973**, *58*, 4496.
(74) Baerends, E. J.; Ellis, D. E.; Ros, P. *Chem. Phys.* **1973**, *2*, 41.
(75) Dunlap, B. I.; Connolly, J. W. D.; Sabin, J. R. *J. Chem. Phys.* **1979**, *71*, 3396.
(76) Van Alsenoy, C. *J. Comput. Chem.* **1988**, *9*, 620.
(77) Weigend, F.; Haeser, M. *Theor. Chem. Acc.* **1997**, *97*, 331.
(78) Neese, F. N. *J. Chem. Phys.* **2003**, *119*, 9428–9443.
(79) Frisch, M. J. et al. *Gaussian 03*, Revision E.01; Gaussian, Inc.: Wallingford, CT, 2004.
(80) Becke, A. D. *J. Chem. Phys.* **1993**, *98*, 5648–5652.
(81) Becke, A. D. *J. Chem. Phys.* **1993**, *98*, 1372–1377.
(82) Lee, C. T.; Yang, W. T.; Parr, R. G. *Phys. Rev. B: Condens. Matter* **1988**, *37*, 785–789.
(83) Greene, S. N.; Richards, N. G. J. *Inorg. Chem.* **2006**, *45*, 17–36.
(84) Tannor, D. J.; Marten, B.; Murphy, R.; Friesner, R. A.; Sitkoff, D.; Nicholls, A.; Ringnalda, M.; Goddard, W. A., III; Honig, B. *J. Am. Chem. Soc.* **1994**, *116*, 11875–11882.
(85) Tissandier, M. D.; Cowen, K. A.; Feng, W. Y.; Gundlach, E.; Cohen, M. H.; Earhart, A. D.; Tuttle, T. R.; Coe, J. V. *J. Phys. Chem. A* **1998**, *102*, 7787–7794.
(86) Tawa, G. J.; Topol, I. A.; Burt, S. K.; Caldwell, R. A.; Rashin, A. A. *J. Chem. Phys.* **1998**, *109*, 4852–4863.

Scheme 1

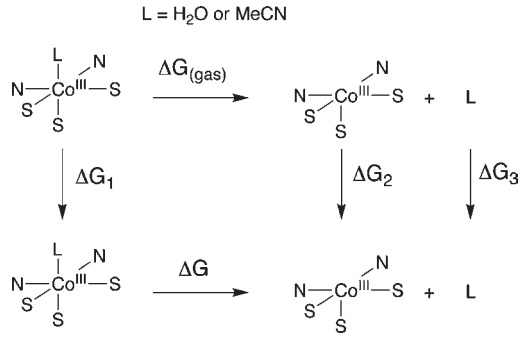

Scheme 2

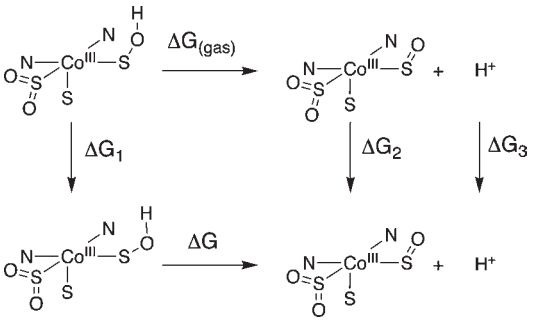

Scheme 3

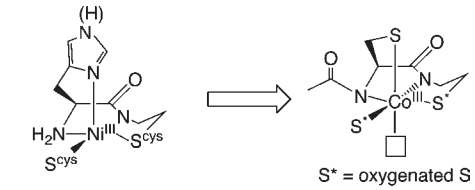

His(1) was changed to a Cys-residue and the free N-terminal amine was capped with an acetyl group yielding the peptide NHase-m1 (AcNH-CCDLP-CGVYD-PA-COOH). Capping the N-terminal group with an acetyl group provides the cobalt center with the requisite bis-amidate ligand set, which will also promote sulfur-based oxygenation.[87]

Addition of 1 equiv of $CoCl_2$ to solutions of NHase-m1 (10 mM NEM buffer, pH = 8.0) instantly forms a green solution. The UV−vis-NIR spectrum of the Co^{II} metallopeptide (Figure 2 and Supporting Information) in D_2O NEM buffer (10 mM, pD = 8.0) displays ligand field bands in the vis−NIR spectrum between 5,300−10,500 cm^{-1} (1,890−952 nm) and 11,800−18,350 cm^{-1} (850−545 nm) and more intense charge transfer bands in the UV-region at 29,325 and 36,495 cm^{-1} (341 and 274 nm) (Figure 2). The higher-energy ligand-field bands display evidence of splitting due to spin−orbit coupling effects, consistent with tetrahedral Co^{II}. All of these visible absorption bands are CD active demonstrating the Co-ion is ligated to the apo-peptide forming "[Co^{II}NHase-m1]" (Supporting Information). On the basis

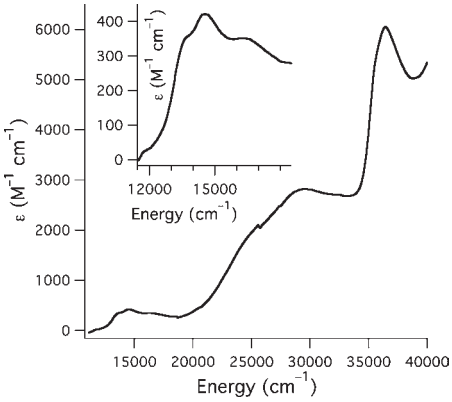

Figure 2. Electronic absorption spectrum of Co^{II} ligated NHase-m1. The inset depicts an expansion of the higher-energy ligand-field transitions.

of the overall broad-shapes of the $^4T_1(F) \leftarrow {}^4A_2(F)$ and $^4T_1(P) \leftarrow {}^4A_2(F)$ transitions (from T_d parentage) we can surmise that the Co^{II} center is contained in a mixture of ligand environments ranging from a $Co^{II}N_2S_2$ to a $Co^{II}S_4$ ligand environment.[88] This may be expected as the peptide NHase-m1 was not designed to hold a metal ion in a tetrahedral geometry; thus, the cobalt ion is ligated in a non-distinct ligand environment by one or more NHase-m1 peptides. In contrast, oxidation of cobalt to the Co^{III} oxidation state yields one distinct ligand environment for cobalt within NHase-m1 (vide infra).

Formation of [Co^{III}NHase-m1]. Exposure of solutions of [Co^{II}NHase-m1] to air results in the gradual formation of a brown solution (Supporting Information). This color change is consistent with the oxidation of the Co^{II} ion to a thiolate-ligated Co^{III} ion over the period of 10 min.[33,42,91−93] Despite the fact that the cobalt center is oxidized over a relatively short period of time, the full formation of the catalytically active species is only achieved after 3 h of maturation under air exposure (see nitrile hydrolysis subsection). Following the 3 h maturation time, solutions of the oxidized metallopeptide are purged with argon and handled using air-free techniques.

Mature [Co^{III}NHase-m1] was first examined by gel-permeation chromatography (GPC) and ESI-MS. GPC data were recorded at 350 nm, where the free peptide does not absorb, and show a single peak at 7.24 min, which equates to a molecular mass of 1395 g mol^{-1} (Supporting Information). ESI-MS data are most consistent with several oxygen atoms covalently attached to the metallopeptide. The most prominent peak in the ESI-MS corresponds to NHase-m1 (minus the five protons required for Co^{III} ligation) with three additional oxygen atoms (m/z = 1339), while the second most prominent peak corresponds to the peptide with two additional oxygen atoms (m/z = 1323). The other two peaks observed correspond to Co-coordinated NHase-m1 with three oxygen atoms

(87) Shearer, J.; Dehestani, A.; Abanda, F. *Inorg. Chem.* **2008**, *47*, 2649–2660.

(88) Reddi, A. R.; Guzman, T. R.; Breece, R. M.; Tierney, D. L.; Gibney, B. R. *J. Am. Chem. Soc.* **2007**, *129*, 12815–12827.

(89) Shearer, J.; Callan, P. E., unpublished results.

(90) Buonomo, R. M.; Font, I.; Maguire, M. J.; Reibenspies, J. H.; Tuntulani, T.; Darensbourg, M. Y. *J. Am. Chem. Soc.* **1995**, *117*, 963–973.

(91) Elder, R. C.; Kennard, G. J.; Payne, M. D.; Deutsch, E. *Inorg. Chem.* **1978**, *17*, 1296–1303.

(92) Lydon, J. D.; Elder, R. C.; Deutsch, E. *Inorg. Chem.* **1982**, *21*, 3186–3197.

(93) Shearer, J.; Kung, I. Y.; Lovell, S.; Kaminsky, W.; Kovacs, J. A. *J. Am. Chem. Soc.* **2001**, *123*, 463–468.

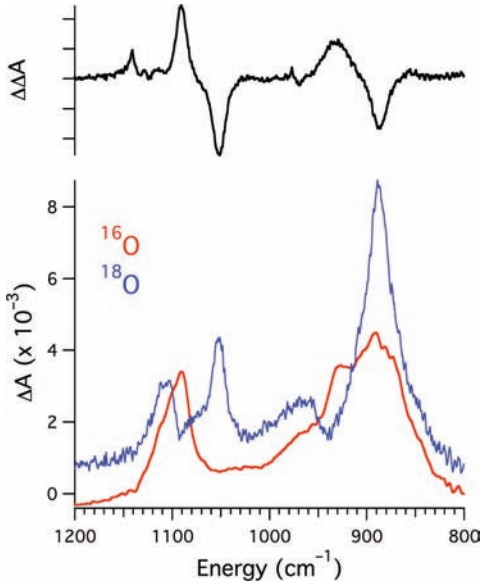

Figure 3. Bottom: FTIR spectra of [Co^{III}NHase-m1] matured in the presence of $^{16}O_2$ (red) versus $^{18}O_2$ (blue) gas. Top: Difference spectrum.

associated with the metallopeptide (m/z = 1398) followed by the metallopeptide with two oxygen atoms associated with the peptide (m/z = 1381).

FTIR Spectroscopy. FTIR spectra were recorded with an ATR device on partially dehydrated films of [Co^{III}NHase-m1]. To simplify the analysis of the resulting data the FTIR spectrum of the apo-peptide was used as a background. The resulting FTIR data yielded peaks in the region where metal-coordinated Cys-SO_2 (1150−1075 cm^{-1}) and Cys-SO (1000−850 cm^{-1}) moieties should be observed (Figure 3).[17,95] We note that these peaks overlap with other IR active vibrational modes that were not fully accounted for in the apo-peptide background spectrum.

To both confirm the presence of coordinated oxygenated cysteinates and determine their corresponding energies, we matured [Co^{III}NHase-m1] in the presence of $^{18}O_2$ gas. The resulting difference spectrum showed a disappearance of the peaks at 1091 and 928 cm^{-1} from the $^{16}O_2$ matured spectrum and the appearance of peaks at 1052 and 889 cm^{-1} (Figure 3). This is consistent with what would be expected from a simple Hooke's Law relationship of changing a S=^{16}O harmonic oscillator to a S=^{18}O harmonic oscillator. There are also small bands that occur at approximately 1130 cm^{-1}, which are attributable to the formation of a small amount of the corresponding bis-sulfinate species (vide infra). These are the only IR active bands that are sensitive to isotopic substitution in the region of the IR spectrum where SO_x stretching modes are observed. As such, these features are consistent with a mixture of Co-coordinated Cys-SO_2 and Cys-SO ligands as the major product following 3 h of air exposure.[17,37,90,95−98] Furthermore, these peaks appear where the Cys-SO_2 and Cys-SO asymmetric stretches in FeNHase appear following photorelease of NO.[17] Our findings of the mixed cysteinate/Cys-SO_2/Cys-SO coordination motif are supported by preliminary S K-edge studies performed on matured [Co^{III}NHase-m1].[89]

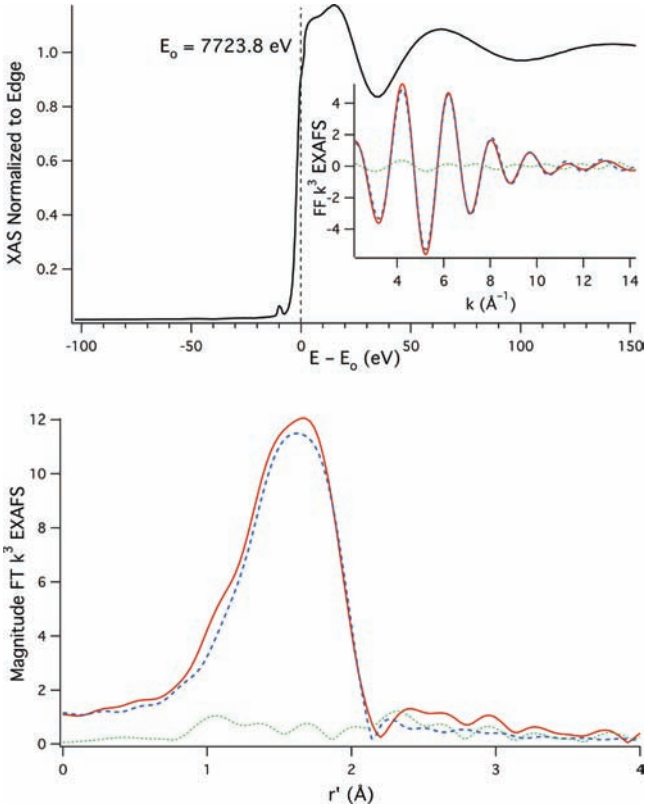

Figure 4. Top: XANES region of the X-ray absorption spectrum of [Co^{III}NHase-m1] following 3 h of maturation. Inset depicts the FF k^3 data (Fourier Transformed from 2.2−14.2 k; back-transformed from 0.8 to 2.5 Å). Bottom: FT k^3 data. In both the FT and FF k^3 data the real data is represented as the solid red lines, the simulated data is depicted as the dashed blue line, and the difference spectra are depicted as the dashed green line. Best fits to the data: 3 N/O scatterers (1.93 Å σ^2 = 0.0062(8)$Å^2$), 2 S scatterers (2.21 Å σ^2 = 0.0037(3)$Å^2$); ε^2 = 0.82.

Surprisingly, we also find that the 928 cm^{-1} peak is sensitive to H/D exchange (Supporting Information). Recording the IR spectrum from a peptide matured in D_2O buffer (10 mM NEM, pD = 8.0) leads to a shift of this peak from 928 cm^{-1} to ~900 cm^{-1}. These data strongly suggest that the Cys-S=O moiety is protonated (Cys-S=O(H)).

Co K-Edge X-ray Absorption Spectroscopy. Co K-edge X-ray absorption spectroscopy was utilized to probe the coordination environment about the Co-center of [Co^{III}NHase-m1] (Figure 4). The pre-edge region displays a weak pre-edge feature that is assigned to a Co(1s → 3d) transition. This transition is formally dipole forbidden, but can gain intensity in non-centrosymmetric coordination environments through the mixing of 4p-character into the final state.[99] Thus, the area under this peak can be compared with other complexes to estimate the coordination number about the cobalt center. We find that the area of this peak (6.8 eV relative to the edge height) is

(94) Tyler, L. A.; Noveron, J. C.; Olmstead, M. M.; Mascharak, P. K. *Inorg. Chem.* **2000**, *39*, 357–362.
(95) Grapperhaus, C. A.; Darensbourg, M. Y. *Acc. Chem. Res.* **1998**, *31*, 451–459.
(96) Masitas, C. A.; Mashuta, M. A.; Grapperhaus, C. A. *Inorg. Chem.* **2010**, *49*, 5344–5346.
(97) Tyler, L. A.; Olmstead, M. M.; Mascharak, P. K. *Inorg. Chem.* **2001**, *40*, 5408–5414.
(98) Farmer, P. J.; Verpeaux, J. N.; Amatore, C.; Darensbourg, M. Y. *J. Am. Chem. Soc.* **1994**, *116*, 9355–9356.
(99) Westre, T. E.; Kennepohl, R.; DeWitt, J. G.; Hedman, B.; Hodgson, K. O.; Solomon, E. I. *J. Am. Chem. Soc.* **2007**, *119*, 6297–6314.

intermediate between a five and a six coordinate Co^{III} center, as was previously observed in the X-ray absorption spectrum of CoNHase (area = 6.3 eV).[100]

The EXAFS region of the Co K-edge X-ray absorption spectrum is also consistent with what had been previously observed for CoNHase.[100,101] We obtain a best-fit to the EXAFS data using a *five* coordinate model with the Co-center coordinated by two S-scatterers at 2.21 Å and three N/O scatterers at 1.93 Å. These data could also be refined for a five coordinate model with three S-scatterers at 2.22 Å and two N/O scatterers at 1.97 Å with only a moderate increase in both the error to the data refinement (ε^2 = 0.82 vs 0.93) and the S Debye−Waller parameter (σ^2 = 0.0037(3)Å^2 vs 0.0086(5)Å^2). Similar to CoNHase, we also find a statistically valid fit to the EXAFS data for six coordinate models. When the EXAFS data for [Co^{III}NHase-m1] is modeled as an $S_2(N/O)_4$ environment there is a slight modification to the refined bond-lengths with two S-scatterers at 2.24 Å and four N/O scatterers at 1.93 Å. Despite the slight increase in the error of the EXAFS fit (ε^2 = 0.82 vs 1.06) there is a dramatic increase in the refined Debye−Waller parameter for the N/O scatterers (σ^2 = 0.0062(8)Å^2 vs 0.022(5)Å^2), making this six-coordinate model unlikely. Likewise, the $S_3(N/O)_3$ model yielded a valid fit to the data, but the Debye−Waller factors for both the S and N/O scatterers became unrealistically large (∼ 0.015 Å^2). Of all four models considered above the $S_3(N/O)_2$ model yielded a bond valence sum that was most consistent with Co(III) (3.19 vs an optimal value of 3.00)[51] with the other refinements yielding bond valence sums that ranged from 3.30−3.70. Thus, the $S_3(N/O)_2$ is the most consistent formulation for the coordination environment of [Co^{III}NHase-m1]. It should also be noted that overall the EXAFS data for [Co^{III}NHase-m1] compare well with fits to the EXAFS data originally recorded for CoNHase.[101] Thus, it appears that the coordination environment about [Co^{III}NHase-m1] is similar to the coordination environment about CoNHase/SCNase (Figure 1).

Electronic Absorption and CD Spectroscopy. The electronic absorption spectrum of [Co^{III}NHase-m1] is consistent with what has been previously observed for CoNHase and other low-spin thiolate-ligated Co^{III} complexes (Figure 5).[33,42,91−94] The spectrum is relatively featureless with a gradual increase in absorbance from 11,500 to 20,000 cm^{-1} (870−500 nm), shoulders at 22,125 (452 nm) and 28,735 cm^{-1} (348 nm), and a defined peak at 35,460 cm^{-1} (282 nm). The CD spectrum (Figure 5) of the oxidized Co-metallopeptide is also consistent with CoNHase; however, the signs of the resulting low energy bands are different than observed in the metalloenzyme.[102] This can be largely rationalized by the fact that the Co^{III} centers contained within NHase-m1 versus NHase are in different chiral environments thus leading to different CD properties. These data are displayed in Figure 5 and Table 1.

The lowest four energy bands are derived from d → d transitions. From these data it is instantly apparent that

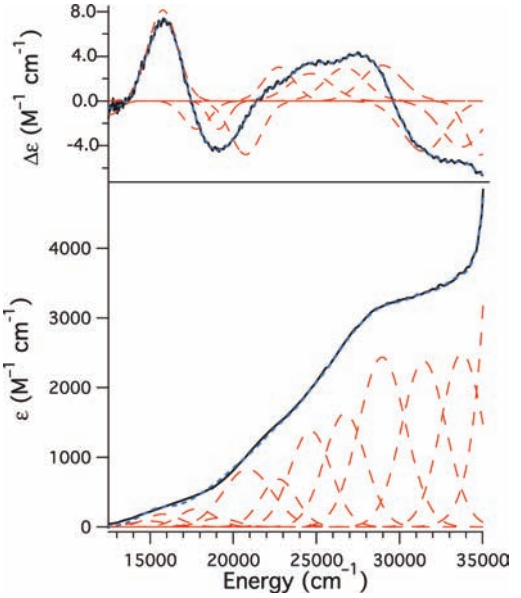

Figure 5. CD (top) and electronic absorption spectra (bottom) of [Co^{III}NHase-m1] obtained in 10 mM NEM buffer at a pH = 8.0. The black solid spectrum represents the experimental data, the dashed red peaks represent the best-fit of the absorption and CD spectra decovolved into Gaussian line shapes, and the dashed blue spectrum represents the best-fit of the absorption and CD spectrum resulting from the sum of the Gaussian line shapes.

the complex cannot be described as arising from *O* symmetry; values obtained for the Racha B parameter and $10D_q$ are unreasonably small for low-spin Co^{III}. Instead, the data are consistent with a complex arising from D_4 (or C_4) parentage. For transitions to be CD active they must be both electronically and magnetically dipole allowed. The anisotropy factor, g ($g = |\Delta\varepsilon|/\varepsilon$), is a sensitive measure for judging if a transition is magnetically dipole allowed; if g is greater than 0.01 the transition can be considered magnetically dipole allowed.[103] For [Co^{III}NHase-m1] the lowest energy transition has a g = 0.004 while the next three transitions all have $g > 0.01$ (Table 1). In the case of states derived from D_4 parentage the lowest energy transition, the $^1B_2 \leftarrow {}^1A_1$ transition, is magnetically dipole forbidden. In contrast the next three highest energy transitions are magnetically dipole allowed (i.e., the $^1E \leftarrow {}^1A_1$, $^1A_2 \leftarrow {}^1A_1$, and $^1E \leftarrow {}^1A_1$). Thus, the CD and absorption data are most consistent with the Co^{III} center contained within either a square-pyramidal five-coordinate or tetragonally distorted six-coordinate ligand environment. We suggest that the five-coordinate species is most likely (vide infra, vide supra).

Nitrile Hydrolysis By [Co^{III}NHase-m1]. Nitrile hydrolysis studies were performed in aqueous buffer (10 mM NEM; pH 8.0) by the addition of 1 equiv of [Co^{III}NHase-m1] to 100 equiv of nitrile (10 mM nitrile was used). Reactions were run for 18 h at 25 or 50 °C in sealed NMR tubes under an atmosphere of argon. The nitriles that were investigated included: acetonitrile, 3-cyanopyridine, and acrylonitrile. In the case of 3-cyanopyridine no nitrile hydrolysis was observed under any conditions. When acetonitrile is used as a substrate only trace amounts of

(100) Brennan, B. A.; Alms, G.; Nelson, M. J.; Durney, L. T.; Scarrow, R. S. *J. Am. Chem. Soc.* **1996**, *118*, 9194–9195.

(101) Our reanalysis of the EXAFS data for CoNHase presented in ref 92 shows a valid solution for a five coordinate $(N/O)_2S_3$ model.

(102) Payne, M. S.; Wu, S.; Fallon, R. D.; Tudor, G.; Stieglitz, B.; Turner, I. M., Jr.; Nelson, M. J. *Biochemistry* **1997**, *36*, 5447–5454.

(103) Johnson, M. K. In *Physical Methods in Bioinorganic Chemistry; Spectroscopy and Magnetism*; Que, L., Jr., Ed.; University Science Books: Sausalito, CA, 2000; pp 233−285.

Table 1. Spectral Parameters Obtained from the Simultaneous Deconvolution of the Electronic Absorption and CD Spectra of Fully Matured [Co^{III}NHase-m1]

peak	energy (cm^{-1})	ε (M^{-1} cm^{-1})	$\Delta\varepsilon$ (M^{-1} cm^{-1})
1	12,602	30	−0.12
2	15,766	80	8.13
3	17,794	140	−2.50
4	19,135	235	−2.51
5	20,842	825	−4.79
6	22,813	685	3.03
7	24,621	1,370	2.46
8	26,663	1,630	2.98
9	29,015	2,440	3.19
10	31,686	2,380	−4.36
11	33,744	2,490	−4.08
12	34,813	N/A[a]	−4.83

[a] This peak could not be deconvoluted in the electronic absorption spectrum because of an intense feature at ~38,000 cm^{-1}.

Table 2. Turnover Numbers Following 18 h of Reaction Time Per [Co^{III}NHase] as a Function of Air Exposure Time

air exposure time (min)	turnover number
0	ND[a]
10	ND[a]
60	12(2)
120	36(2)
180	58(4)
240	17(1)
300	ND[a]
360	ND[a]

[a] ND: nitrile hydrolysis was not detected.

acetamide (0.6 equiv per [Co^{III}NHase-m1]) could be detected by GC/MS after 18 h of reaction time at 50 °C.

In contrast to these two nitriles, the sterically unencumbered and *activated* nitrile acrylonitrile was readily converted into acrylamide. We observe that up to 58 turnovers of acrylonitrile to acrylamide could be effected by [Co^{III}NHase-m1] at 25 °C over 18 h. Control experiments of buffer, 0.1 mM [$Co^{III}(NH_3)_6$](3Cl^-), or the NHase-m1 apo-peptide yielded no evidence of nitrile hydrolysis.

The hydrolysis of acrylonitrile to acrylamide is highly dependent upon the maturation time of [Co^{III}NHase-m1] (i.e., the exposure time of the metallopeptide solution to air prior to purging the solution with argon). If the metallopeptide solution is exposed to air for only 10 min and then purged with argon no acrylonitrile hydrolysis is observed. As one extends the maturation time the amount of nitrile hydrolysis dramatically increases, with an optimal maturation time of 3 h observed for [Co^{III}NHase-m1]. Following 3 h of air maturation there is a precipitous decrease in acrylonitrile hydrolysis, with no acrylonitrile hydrolysis observed following 5 h of maturation (Table 2). This strongly suggests that there is a slow activation process followed by a more rapid deactivation process effected by O_2.

Identification of the Active Form of [Co^{III}NHase-m1]. From the above acrylonitrile hydrolysis experiments it seems a reasonable supposition that the active form of [Co^{III}NHase-m1] is obtained only after relatively extensive oxidation by O_2. Because of the rapid oxidation of Co^{II} to Co^{III},[104] this suggests that slow sulfur based oxidation may be the reason for the low activity of the not fully matured [Co^{III}N Hase-m1]. To quantify the changes in sulfur based oxygenation of [Co^{III}NHase-m1] versus maturation time we examined the FTIR spectrum of the metallopeptide as a function of air exposure time (Figure 6, Supporting Information). After 10 min of air maturation only the bands corresponding to a sulfinate species are present, with bands observed between 1120−1060 cm^{-1}.[95] Over the course of 3 h the band corresponding to the sulfenate begins to appear at 928 cm^{-1}, with the maximum in absorbance of this transition reached after approximately 3 h. Following 3 h of maturation the band corresponding to the sulfenate disappears, and is completely absent after 5 h [Co^{III}NHase-m1] of air exposure. Concurrent with the disappearance of the sulfenate stretch is the appearance of additional stretching modes at 1073 and 1127 cm^{-1}, suggesting the formation of a bis-sulfinate coordinated Co^{III} center.[95] A bis-sulfinate species appears to be the end sulfur-based oxygenation product of Co^{III} and Fe^{III} coordination compounds reminiscent of NHase; such products are observed in both SCNase, NHase, and small molecule Co- and Fe-NHase biomimetic complexes.[1,10,15,37] Furthermore, there is good experimental evidence that the bis-sulfinate form of SCNase is catalytically inactive,[10] which is what we observe in our NHase biomimetic compound. *From our data it thus appears that the active form of* [Co^{III}*NHase-m1*] *has one sulfinate and one protonated sulfenate coordinated to the* Co^{III} *center* (Scheme 4).

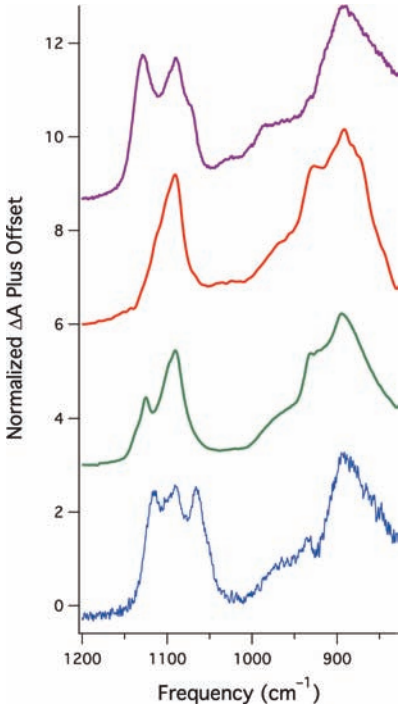

Figure 6. Infrared spectra of [Co^{III}NHase-m1] recorded after 10 min (blue), 1 h (green), 3 h (red), and 5 h (purple) of exposure to air. Difference spectra are reported in the Supporting Information.

(104) Analysis of the NIR region of the electronic absorption spectrum of [Co^{III}NHase-m1] following 10 min of air maturation shows the complete disappearance of the low energy Co^{II} $^4T_1(F) \leftarrow {}^4A_2(F)$ transition demonstrating the complete oxidation of Co^{II} to Co^{III} in this time frame.

(105) Hashimoto, K.; Suzuki, H.; Taniguchi, K.; Noguchi, T.; Yohda, M.; Odaka, M. *J. Biol. Chem.* **2008**, *283*, 36617–36623.
(106) Mitra, S.; Holz, R. C. *J. Biol. Chem.* **2007**, *282*, 7397–7404.
(107) Rao, S.; Holz, R. C. *Biochemistry* **2008**, *47*, 12057–12064.

Scheme 4

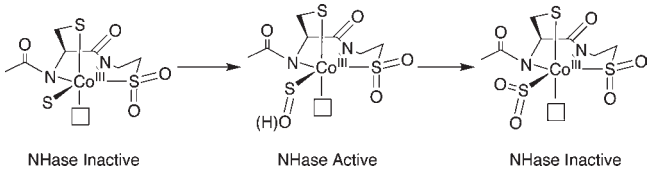

Table 3. Co^{III} Bond Lengths Obtained from the Electronic Structure Calculations for Selected Computational Models (mPWPW91/aug−cc−TZVPP)

model	Co−S Å[a]	Co−S Å[b]	Co−S Å	Co−N Å[c]	Co−N Å	Co−O Å
2	2.220	2.170	2.223	1.975	1.950	N/A
2−H_2O	2.229	2.177	2.233	1.989	1.954	2.106
3	2.228	2.167	2.235	1.980	1.969	N/A
3−H_2O	2.227	2.216	2.283	1.996	1.976	2.070
4	2.219	2.159	2.243	1.965	1.888	N/A
4−H_2O	2.265	2.191	2.270	1.992	1.918	2.114
5	2.229	2.119	2.232	1.984	1.941	N/A
5−H_2O	2.282	2.241	2.292	2.003	1.972	2.080

[a] Thiolate *trans* to the water or vacant-site. [b] Sulfinate. [c] Amidate nitrogen *trans* to the sulfinate.

Computational Analysis

To further probe the identity of the active species a series of computational models were constructed based on the predicted active-site structure of [Co^{III}NHase-m1]. The electronic absorption, CD, and IR spectra of these complexes were then calculated and compared with the available experimental data for [Co^{III}NHase-m1] described above. All of the models involved coordinating a Co^{III} ion to an AcN-Cys-Cys-H bis-peptide, an equatorial ethanethiol, and an additional axial ligand. Subsequent sulfur-based oxidation and sulfenate protonation was then examined.

Description of Computational Models. Of the 15 computational models considered, stationary points along the potential energy surface could only be located for 13; in the case of the computational model with no oxygenated sulfurs ($(Co\text{-}NHase)^{2-}$; **1**) only the 5 coordinate complex was found to be a stationary point. For the oxygenated computational models, both 5 coordinate, MeCN, and H_2O bound forms could be successfully located. Structures of the computational models and their relevant metrical parameters are displayed in Chart 2 and Table 3, respectively.

Surprisingly, all of the five coordinate computational models investigated containing oxygenated sulfur atoms were found to possess singlet ground states. The higher spin-states (triplet and quintet spin states) were found to be ~4,000 cm^{-1} higher in energy than the low-spin complexes. This is a direct result of sulfur-based oxygenation, which renders the sulfur π based AOs unavailable for bonding with the cobalt π-type AOs. As a consequence of the strong σ bonding along the molecular *x*, *y*, and *z* axis from the anionic ligands, there is a significant destabilization of the Co($3d_{x^2-y^2}$) and Co($3d_{z^2}$). Relatively poor π-donation from the amides to the Co(3d(π)) orbitals leads to only a small destabilization of these d-type orbitals (Figure 7). It should be noted that these five coordinate complexes also yielded Co−S and Co−N bond lengths that best matched the EXAFS data obtained for [Co^{III}NHase-m1], with Co−S bond lengths ranging between 2.21−2.26 Å and Co−N bond lengths ranging between 1.90−1.98 Å (Table 3).

Calculated versus Experimental IR Spectra. IR spectra were calculated for all stationary points with both $^{16}O_2$ and $^{18}O_2$ labeled oxygenated sulfurs (Table 4). Of these an excellent match between the experimental data obtained for [Co^{III}NHase-m1] and the calculated IR data was obtained for the five-coordinate *protonated*-sulfenate/sulfinate ligated computational model **4** ($(Co\text{-}NHase\text{-}SO_2/SO(H))^-$) (Figure 8, Table 4). The calculated spectrum displays $^{16}O_2$═S and H−^{16}O═S stretches at 1093 and 930 cm^{-1}, respectively, that red-shift to 1056 and 881 cm^{-1} upon ^{18}O substitution. The calculated IR spectrum for the corresponding six-coordinate water ligated **4-H_2O** ($(Co\text{-}NHase\text{-}SO_2/SO(H)\text{-}H_2O)^-$) displays a $^{16}O_2$═S stretch at 1154 cm^{-1} and an H−^{16}O═S stretch at 1051 cm^{-1}, which are both much to high in energy to be consistent with the experimental data. The unprotonated complex **3-H_2O** is an even poorer match to the experimental data with $^{16}O_2$═S stretches at 1232/1073 cm^{-1} and an ^{16}O═S stretch at 1179 cm^{-1}. We note that the calculated IR spectrum for the five coordinate monosulfinate complex **2** ($(Co\text{-}NHase\text{-}SO_2)^{2-}$) matches well with the IR data obtained for [Co^{III}NHase-m1] following 10 min of maturation, while the bis sulfinate computational model **5-H_2O** ($(Co\text{-}NHase\text{-}2(SO_2)\text{-}H_2O)^{2-}$) has $^{16}O_2$═S stretches that match well with the IR data

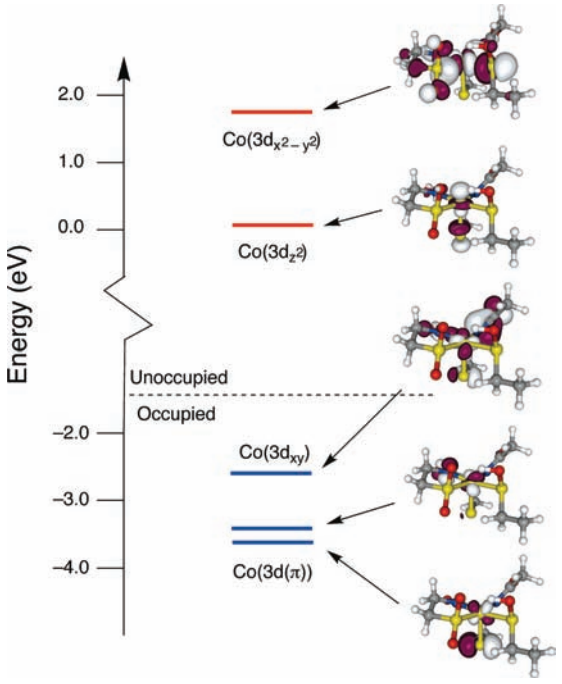

Figure 7. Energy level diagram of the Co(3d) orbitals depicting the occupied (blue) and unoccupied (red) orbitals. Iso-surface plots of the corresponding molecular orbitals were generated with the molecular graphics program Molkel.

Table 4. Vibrational Data Obtained for [Co^{III}NHase-m1] and Selected Computational Models for the Sulfinate and Sulfenate S═O Stretching Energies (mPWPW91/aug−cc−TZVPP)

compound	S═$^{16}O_2$ (cm^{-1})	S═$^{18}O_2$ (cm^{-1})	S═^{16}O (cm^{-1})	S═^{18}O (cm^{-1})
[Co^{III}NHase-m1]	1091	1052	928	889
2	1098	1060	N/A	N/A
	1023	982		
3	1081	1056	1044	1005
3−H_2O	1232	1209	1179	1131
	1073	1028		
4	1093	1056	930	881
4−H_2O	1154	1121	1051	1010
	1126	1094		
5−H_2O	1131	1096	N/A	N/A
	1120	1087		
	1082	1045		
	1064	1033		

(108) Barondeau, D. P.; Kassmann, C. J.; Bruns, C. K.; Tainer, J. A.; Getzoff, E. D. *Biochemistry* **2004**, *43*, 8038–8047.
(109) Wuerges, J.; Lee, J.-W.; Yim, Y.-I.; Yim, H.-S.; Kang, S.-O.; Carugo, K. D. *Proc. Natl. Acad. Sci. U. S. A.* **2004**, *101*, 8569–8574.

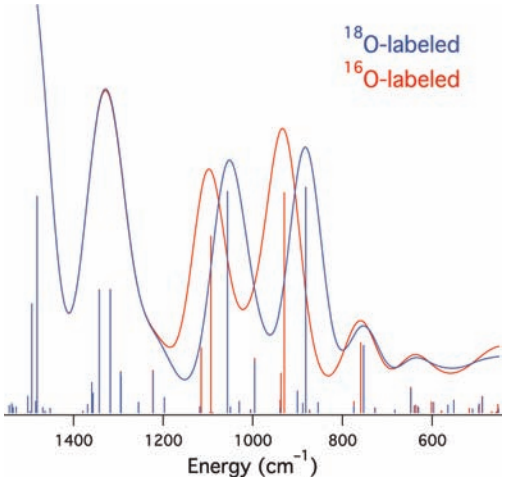

Figure 8. Simulated IR spectrum of **4** with ^{16}O (red) and ^{18}O (blue) labeling of the sulfinate and sulfenate. The sticks represent the individual transitions, and the spectra was generated by applying Gaussian line shapes (50 cm^{-1} peak width) to the transitions and summing them together.

obtained for [Co^{III}NHase-m1] following 5 h of air exposure. These data are summarized in Table 4.

Excited State Calculations and Comparison With Experimental Electronic Absorption and CD Spectra. The electronic absorption and CD spectra experimentally obtained for [Co^{III}NHase-m1] were compared to the calculated spectra of **3-H_2O**, **4**, **4-H_2O**, and **5-H_2O** (Figure 9 and Supporting Information). The aqua-complexes of **3** and **5** as well as five-coordinate **4** were examined as these represent minima along the potential energy surface (vide infra), while **4-H_2O** was examined for comparison with the other six-coordinate aqua-complexes. All excited state calculations employed Neese's spectroscopically oriented configurational interaction (SORCI) methodology.[78] Unlike time-dependent DFT, the SORCI method is a true multiconfigurational ab initio method, and therefore takes into account the multiconfigurational nature of the excited and ground states. Although this is most important for open shell systems, we and others have found that the SORCI method can be more accurate in reproducing the electronic spectra of closed shell systems than other more widely used excited state methods.[78,110−112] A full account of the theory behind the SORCI method can be found in reference 78.

In this study we used a moderately−large sized CAS(8,8) active space to examine the first five spin allowed transitions of the four computational models (Figure 9, Supporting Information). The simulated and experimental electronic absorption data are rather indistinct, as would be expected for low-spin Co^{III}. In contrast the simulated and experimental CD spectra are rather illuminating. For all six coordinate computational models considered the simulated CD spectra do not match that of the experimental data well in terms of both transition energies, rotational strengths, and signs. For these, the lowest energy transition corresponds to a nominal Co(3d(π)) → Co($3d_{x^2-y^2}$) transition, which occur at relatively high energies (~17,000 cm^{-1}) when compared to the experimental data. Although a ~5,000 cm^{-1} blue-shift in calculated versus experimental data may be expected for methods such as TD-DFT, the SORCI methodology is not typically this inaccurate. Furthermore, the calculated Co(3d(π)) → Co($3d_{x^2-y^2}$) transition has a large rotational strength, and is negatively signed, which is

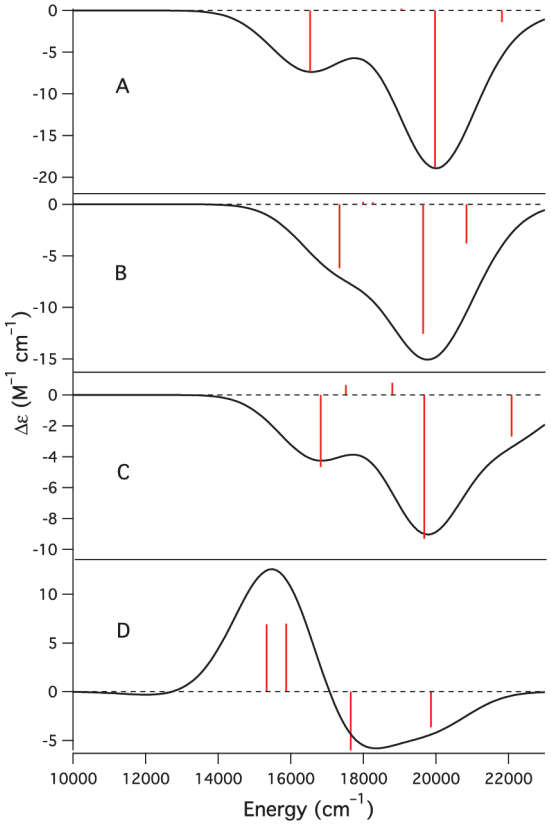

Figure 9. Simulated CD spectra for **2-H_2O** (A), **3-H_2O** (B), **4-H_2O** (C), and **4** (D). Simulated spectra are sums of Gaussian lineshapes applied to the individual transitions (red sticks) using a 1500 cm^{-1} peak width.

inconsistent with the experimental data. The next two transitions for the six-coordinate models considered are weak and positively signed, while the fourth and fifth are stronger than the first and are negatively signed. This leads to an overall low energy region of the CD spectrum that does not match the experimental data well for any of the computationally derived aqua-species. It should be noted that the CD spectrum of [Co^{III}NHase-m1] following extended O_2 exposure matches well with these six-coordinate simulated CD spectra (Supporting Information).

In contrast, the calculated spectrum for five-coordinate **4** is an excellent match with the experimental data. The calculated spectrum displays a weak negative signed CD band at 12,857 cm^{-1} corresponding to a nominal Co($3d_{xy}$) → Co($3d_{z^2}$) transition, two strong positively signed transitions corresponding to Co(3d(π)) → Co($3d_{z^2}$) transitions at ~15,500 cm^{-1},[113] an intense negatively signed Co($3d_{xy}$) → Co($3d_{x^2-y^2}$) transition at 17,619 cm^{-1}, and an intense negatively signed Co(3d(π)) → Co($3d_{x^2-y^2}$) transition at 19,866 cm^{-1}. Thus, the low energy region of the computationally derived CD spectrum for **4** matches the overall line shape, transition signs, and energies determined experimentally for [Co^{III}NHase-m1]. Also, the calculated *g* values compare well with those determined experimentally (Supporting Information). The CD spectrum of the five coordinate unprotonated species was also investigated and produced a reasonable match to the experimentally derived CD data, albeit with minor (~500 cm^{-1}) perturbations to the transition energies.

(110) Shearer, J.; Dehestani, A.; Abanda, F. *Inorg. Chem.* **2008**, *47*, 2649–2660.
(111) Kivala, M.; Boudon, C.; Gisselbrecht, J.-P.; Enko, B.; Seiler, P.; Mueller, I. B.; Langer, N.; Jarowski, P. D.; Gescheidt, G.; Diederich, F. *Chem.—Eur. J.* **2009**, *15*, 4111–4123.
(112) Ray, K.; Weyhermueller, T.; Neese, F.; Wieghardt, K. *Inorg. Chem.* **2005**, *44*, 5345–5360.

(113) Because of the lowered symmetry the $^1E \leftarrow {}^1A_1$ band is split into two bands, which would be unresolvable in the experimental CD data.
(114) We arrive at a calculated pK_a of 12.7 for the HO=S. There is a large error associated with this value as it is derived from a combination of experimental and calculated results.

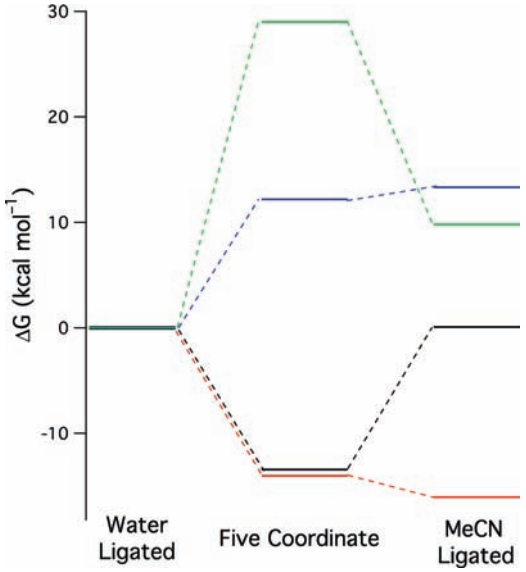

Figure 10. Calculated free energies of ligand exchange normalized to the aqua species **X-H_2O**. The energetics of models **2** (black), **3** (blue), **4** (red), and **5** (green) are depicted.

Energetics of Ligand Displacement from the Co^{III} Center As a Function of Sulfur Oxygenation. The mechanism of substrate hydrolysis by NHase/SCNase remains unresolved; however, one suggested mechanism involves the coordination of the substrate to the metal−center.[8,105−107,115] Because of the sterics about the metal-center in these metalloenzymes such a process must occur through a dissociative mechanism where water (if bound) will dissociate from the M^{III} center and the substrate will coordinate to the vacant site. We therefore examined the energetics of the first two steps of this proposed catalytic mechanism: water dissociation from the Co^{III} center of the computational [Co^{III}NHase-m1] models followed by nitrile (MeCN in this case) association.

Figure 10 displays the computationally derived (B3LYP/aug-cc-TZVPP) free energies associated with each step. Here all energies are zero-point corrected, and are normalized to the corresponding aqua-complexes for comparative purposes. The monosulfinate complex shows a significant energy minima for five-coordinate **2**, which lies 13.45 kcal mol^{-1} lower in energy than the aqua-complex **2-H_2O** and 13.52 kcal mol^{-1} lower in energy than the MeCN ligated complex **2-MeCN**. Thus, **2** would be expected to remain five-coordinate in solution as the equilibrium for either water or nitrile ligation would lie significantly to the left. In contrast, water ligated sulfenate/sulfinate **3-H_2O** is energetically favored because of strong hydrogen bonding to the oxygenated sulfurs; dissociation of the water forming **3** is 12.18 kcal mol^{-1} uphill, while MeCN ligation is 13.33 kcal mol^{-1} higher in energy than the aqua-complex. Protonation of the sulfenate oxygen, forming **4**, significantly destabilizes water hydrogen bonding to the oxidized sulfurs, and thus destabilizes water ligation. Thus, five coordinate **4** is 14.03 kcal mol^{-1} lower in energy than **4-H_2O**. Furthermore, ligation of MeCN to the metal-center forming **4-MeCN** is lower in energy than the five coordinate species, resting 16.05 kcal mol^{-1} below **4-H_2O**. Full oxygenation to the bis-sulfinate ligated compound **5** yields a highly favored aqua-species because of strong hydrogen bonding between the two sulfinate moieties; formation of the five coordinate compound **5** is 29.02 kcal mol^{-1} uphill from the aqua species, while the MeCN compound **5-MeCN** is 9.44 kcal mol^{-1} uphill from the aqua-species. Thus it would appear on the basis of the available spectroscopic and computational evidence that the Co^{III} center of the active-form of [Co^{III}NHase-m1] is five coordinate in aqueous solution. It would also displays a small, but energetically favorable, ability to coordinate nitrile substrates over remaining a five-coordinate species.

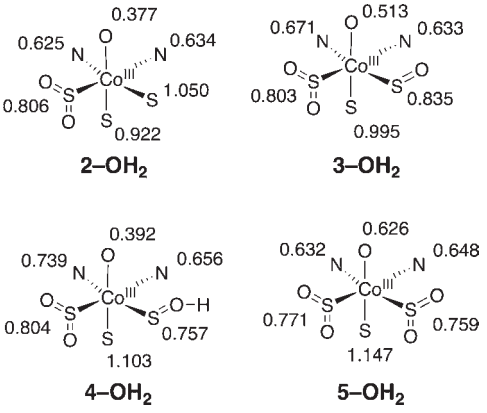

Figure 11. Mayer bond orders (mPWPW91/aug-cc-TZVPP) calculated for the aqua-species **X-H_2O** (**X** = 2, 3, 4, and 5).

Analysis of the Mayer bond order of the aqua-species reveals an interesting trend in bond order as the equatorial thiolate ligands to Co^{III} ions are oxidized (Figure 11).[67−69] Not surprisingly, as the sulfurs become oxidized the Co−S bond order decreases. This is compensated for *not* by an increase in the bond orders of the amide nitrogens *trans* to the oxidized thiolates, but instead an increase by the ligands along the axial bonding vectors. In other words, as the bonding decreases within the *xy* plane it is compensated for by an increase in bonding along the *z*-axis. Thus, a stronger Co^{III}−OH_2 bond is made as the thiolates become sequentially oxidized. The only exception to this trend is the protonated sulfenate complex **4-H_2O**, which has a significantly reduced Co^{III}−O bond-order when compared to unprotonated **3-H_2O** (0.392 vs 0.513), which is a direct result of the destabilization of the water/S=O H−bonding network.

Discussion and Biological Significance

NHases and SCNases are unusual metalloenzymes in that they possess post-translationally modified cysteinate residues coordinated to the active-site metal-ion.[1] It has been widely speculated that these residue modifications are required for catalytic activity; however, the extent of cysteinate oxidation and the reason why NHase and SCNase requires cysteinate oxidation to be catalytically active is still debated.[1,10,14,15,117−119] Using metallopeptide based CoNHase mimic [Co^{III}NHase-m1] in concert with computational models we have demonstrated that a Co^{III} ion contained within a CoNHase-like ligand environment requires the oxidation of one of the cysteinates to a sulfinate and another to a sulfenate for the metallopeptide to display NHase activity. A probable reason for this requirement will be elaborated on below. It must be noted that it is possible that a minor undetectable side product is the catalytically active species. If this were the case, however, its formation and decomposition would have to coincide exactly with the Cys-SO_2/Cys-SO formation within

(115) Preliminary hybrid−DFT studies (B3LYP/TZVP) suggest that nitrile attack by a Co^{III}−bound hydroxide moiety in a ligand environment similar to that found in active [Co^{III}NHase-m1] would proceed with a barrier height of 58.3 kcal mol^{-1}.

(116) Claiborne, A.; Miller, H.; Parsonage, D.; Ross, R. P. *FASEB J.* **1993**, *7*, 1483–1490.
(117) Endo, I.; Odaka, M. *J. Mol. Catal. B: Enzym.* **2000**, *10*, 81–86.
(118) Endo, I.; Nojiri, M.; Tsujimura, M.; Nakasako, M.; Nagashima, S.; Yohda, M.; Odaka, M. *J. Inorg. Biochem.* **2001**, *83*, 247–253.
(119) Endo, I.; Odaka, M. *Prog. Biotechnol.* **2002**, *22*, 159–168.

[Co^{III}NHase-m1]. We would suggest that the likelihood of this situation occurring is low.

Although [Co^{III}NHase-m1] is one of the more active NHase models reported in the literature thus far, its activity is paltry when compared to CoNHase.[6,120] The reduced catalytic activity of [Co^{III}NHase-m1] compared to the NHase metalloenzymes can be readily rationalized. One of the proposed mechanisms of nitrile hydrolysis involves hydroxide (or water) attack of a M^{III}-bound nitrile.[105−107,115] The active-site of [Co^{III}NHase-m1] is sterically crowded owing to the peptide loop composed of residues Cys(2) to Cys(6) (Supporting Information).[108,109] This makes it difficult, if not impossible, for all but the most sterically unencumbered nitriles to coordinate to the metal-center of [Co^{III}NHase-m1]. Therefore, 3-cyanopyridine is not catalytically hydrolyzed by [Co^{III}NHase-m1] because it is likely incapable of coordinating to the Co-center. A similar situation is observed in CoNHase, where 3-cyanopyridine displays a dramatic decrease in activity relative to acrylonitrile,[6,120] because of steric factors.[121]

Other factors besides active-site sterics may also play a part in the reduced catalytic activity of the mimic versus the metalloenzyme. The active-site of [Co^{III}NHase-m1] lacks many of the hydrogen bonding residues from about the NHase active-site that are vital for efficient catalysis.[9,11−15] Therefore only activated nitriles that are already prone to nucleophilic attack will be effectively hydrolyzed by [Co^{III}-NHase-m1], explaining why acrylonitrile is converted to acrylamide catalytically while acetonitrile, an excellent NHase substrate,[6,120] is not hydrolyzed effectively.

We have suggested that the thiolates located in the equatorial plane of [Co^{III}NHase-m1] are the likely candidates for oxidation based on a number of reasons. A computational analysis suggests that the oxidation of the axial thiolate without equatorial oxidation leads to sulfinate dissociation producing a four-coordinate $Co^{III}N_2S_2$ species (Supporting Information), which has been observed experimentally.[32,122] Oxidation of an equatorial Cys to Cys-SO_2 and subsequent oxidation of the axial thiolate will produce a five−coordinate species (Supporting Information). However, the oxidation of the axial thiolate to an SO_x moiety ($x = 1-3$) leads to the exclusive formation of a cobalt O−bound species. Such O−bound complexes have also been observed experimentally.[35,38] Furthermore, these O−bound species all yield calculated S=O IR vibrational modes and CD spectra that are inconsistent with what we observe. Also, our IR data match nicely with what has been observed for NHase, further suggesting that the correct formulation of oxidized cysteinates in [Co^{III}NHase-m1] has been proposed.[17]

We have also presented strong evidence that the sulfenate in [Co^{III}NHase-m1] is protonated. The sulfenate vibrational mode observed for [Co^{III}NHase-m1] is highly sensitive to H/D exchange strongly suggesting that this moiety is protonated under the slightly basic conditions used in this study. This is in line with our computationally derived pK_a of the sulfenate H-OS proton, which is higher than what would be expected by at least 5 orders of magnitude.[114] We reason that the hydrogen bonding between the H−O=S proton and the adjacent sulfinate oxygen raises the sulfenic acid pK_a above the typical range of 3−7[116] in a manner similar to how a proton sponge behaves. We suggest a similar situation exists in NHase (e.g., suflenate protonation or strong Arg hydrogen bonding). This suggestion is supported by computational, FTIR, and XAS studies,[14,16,17,117] and the pH profile of CoNHase, which shows maximum activity at slightly acidic pH.[6]

A number of biological inferences can be made from this work, especially when comparisons are made to results from the biochemical literature. First, there are no *high resolution* crystallographic structures of either NHase or SCNase that lack equatorial cysteinate oxidation. It has been shown from biochemical studies that a Co-chaperone, NhlAE, is responsible for cobalt insertion into apo-NHase through a unique "subunit-swapping" mechanism.[123,124] NhlAE contains three subunits, the α-subunit of CoNHase that contains Co^{III} (in an identical ligand environment as CoNHase) and two NhlE subunits. It was suggested that the NhlE subunits of NhlAE are responsible for both Co-insertion into the α-subunit *and* the oxidation of the cysteinates. Furthermore, it was suggested that the origin of the oxidized cysteine oxygen-atoms was bulk water.[124] Our study cannot comment on the ability of the NhlE subunit of NhlAE to insert cobalt (likely introduced as Co^{II} based on biochemical studies)[124,125] into the NHase α-subunit. However, our study makes it apparent that oxidation of Co^{II} to Co^{III} by O_2 in a ligand environment reminiscent of NHase is facile. Also, using $^{18}O_2$ gas we have demonstrated that the oxygen atoms of SO_2 and SO within a NHase-like coordination motif can easily be derived from O_2. It is thus reasonable to suggest that a similar situation likely exists in both Fe/CoNHase and SCNase, as has been suggested in recent work on sulfur oxidation by isopenicillin-*N*-synthase.[126] Also, it appears that the oxidation of one cysteinate to a sulfinate occurs rapidly after cobalt-insertion, while the second oxidation appears to be considerably slower. Such a finding is consistent with other studies of Co^{III} contained in a NHase-like environment.[10,33,34] Furthermore, our data suggests that the oxidation of the cysteinates is regiospecific; only the equatorial cysteinates appear to be oxidized to sulfinate/sulfenates.

The reason for this regiospecificity has to do with the mechanism of O-atom insertion, which is likely analogous to that observed in Ni-thiolate chemistry.[95,127,128] The oxidation of the cysteine residues likely involves a stepwise mechanisms first involving the coordination of an O_2 molecule to the cobalt−center. Binding of the O_2 negates the problems of molecular oxygen's triplet spin-state, and thus aids the nucleophilic attack of a S-atom toward the bound O_2. This will initially produce a persulfoxidic species, which collapses to a dioxirane. Cleavage of the O−O bond forms the sulfinate

(120) Miyanaga, A.; Fushinobu, S.; Ito, K.; Shoun, H.; Wakagi, T. *Eur. J. Biochem.* **2003**, *271*, 429–438.
(121) Peplowski, L.; Kubiak, K.; Nowak, W. *J. Mol. Model.* **2007**, *13*, 725–730.
(122) Chatel, S.; Rat, M.; Dijols, S.; Leduc, P.; Tuchagues, J. P.; Mansuy, D.; Artaud, I. *J. Inorg. Biochem.* **2000**, *80*, 239–246.
(123) Zhou, Z.; Hashimoto, Y.; Shiraki, K.; Kobayashi, M. *Proc. Natl. Acad. Sci. U. S. A.* **2008**, *105*, 14849–14854.
(124) Zhou, Z.; Hashimoto, Y.; Kobayashi, M. *J. Biol. Chem.* **2009**, *284*, 14930–14938.
(125) Kobayashi, M.; Shimizu, S. *Nat. Biotechnol.* **1998**, *16*, 733–736.
(126) Ge, W.; Clifton, I. J.; Stok, J. E.; Adlington, R. M.; Baldwin, J. E.; Rutledge, P. J. *J. Am. Chem. Soc.* **2008**, *130*, 10096–10102.
(127) Farmer, P. J.; Solouki, T.; Mills, D. K.; Soma, T.; Russell, D. H.; Reibenspies, J. H.; Darensbourg, M. Y. *J. Am. Chem. Soc.* **1992**, *114*, 4601–4605.
(128) Farmer, P. J.; Solouki, T.; Soma, T.; Russell, D. H.; Darensbourg, M. Y. *Inorg. Chem.* **1993**, *32*, 4171–4172.

Scheme 5

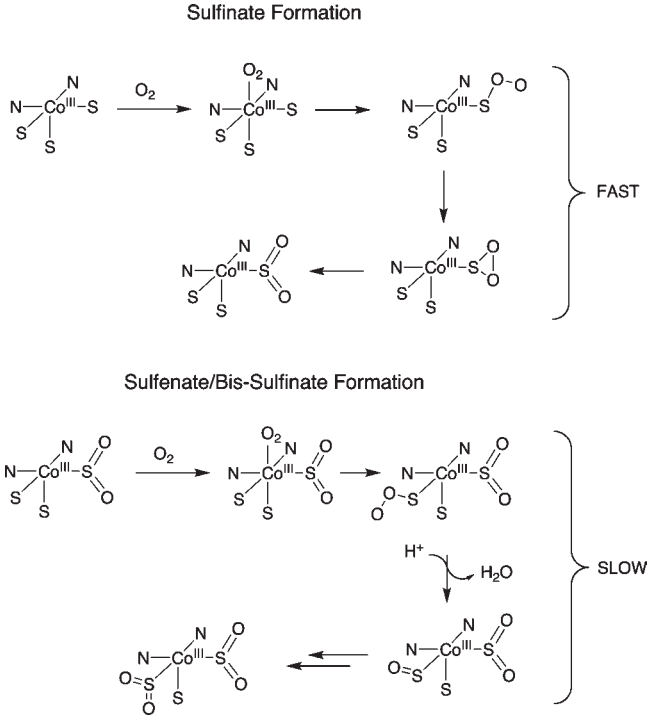

(Scheme 5). The involvement of the Co-center insures that only the equatorial Cys, which is *cis* to the vacant site, will be oxidized, as has been observed by Kovacs in Co^{III}-thiolate chemistry for example.[33] Conversion of the first Cys residue to an Cys-SO_2 will deactivate the nucleophilicity of the other equatorial cysteinate S-atom and dramatically impedes its oxidation.[95] Also, we suggest that because of the reduced nucleophilicity of the S-center the initial persulfoxidic species is heterolytically cleaved in H_2O (prior to potential dioxirane formation) yielding the sulfenate. Additional oxygen atom insertion is slow because of hindered rotation about the Co−S(O)−C bond, making it possible to "trap" the sulfenate before it goes onto the bis-sulfinate species. A similar situation is likely also found in NHase and SCNase, which follows a similar Cys−oxygenation sequence.[10,14,15] We suspect that other factors, such as active-site hydrogen bonding and increased sterics, may further retard bis-sulfenate formation in NHase/SCNase relative to [Co^{III}NHase-m1] making the sulfinate/sulfenate longer lived.

Another important finding of this study is that catalytic activity of [Co^{III}NHase-m1] is only achieved when the equatorial cysteinates are contained in the SO_2 and SO(H) oxidation states. This has been speculated for NHase ever since the first high-resolution crystal-structure of FeNHase appeared in 1998;[14] however, it has never been unambiguously demonstrated. In a previous combined crystallographic/activity study using SCNase the authors suggested that the SO(H) modification is key to SCNase activity; the further oxidation of the Cys-SO ligand to a Cys-SO_2 ligand dramatically reduced (but did not eliminate) the activity of the metalloenzyme.[10] Our evidence strongly suggests that the same occurs in NHase, where the mono and bis-SO_2 forms of our models were inactive. Such a finding is at odds with data suggesting the fully oxygenated metalloenzyme is active, which was based on pure crystallographic evidence.[15]

Lastly our study suggests *why* the SO_2 and SO(H) modifications are necessary. The above presented computational results suggest that when the cysteinates are unoxidized, or only one is oxidized to the mono-SO_2 form, neither substrate nor water coordinating to the Co^{III} center is thermodynamically viable. Oxidation of the other equatorial cysteinate to an SO or SO(H) ligand reduces the electron density being donated to the Co-center by the thiolates, thus allowing for the ligation of an axial ligand. Protonation of the sulfenate to an SO(H) ligand appears to be key in promoting NHase activity. There is a strong hydrogen-bonding network between the Co^{III}−bound H_2O and the oxygens on the two oxidized cysteinates. Protonation of the sulfenate significantly destabilizes water-binding via disruption of the HOH−O═S hydrogen bond. This allows for the facile dissociation of water and subsequent substrate coordination. Full oxygenation of the SO to an SO_2 ligand so strongly favors water binding that a five-coordinate species cannot be generated. A similar situation is observed in the SCNase crystal structure where the fully oxidized bis-SO_2 form of SCNase shows a six-coordinate Co^{III} ion with a water ligand.[10] In the structures of SCNase with the mono-SO_2 ligand or the mono-SO_2 and SO(H) ligand the Co^{III} center is five coordinate with the site *trans* to the unmodified axial cysteinate remaining vacant. Other support for this supposition comes from additional computational and synthetic work on NHase-like metal centers.[16,40,129] We note that it remains to be seen, both on the basis of this study and others, if the SO(H) ligand plays a more intimate role in the NHase catalytic-cycle (such as proton shuttling to the substrate)[129,130] beyond the tuning of the metal-center electronics.

Acknowledgment. The authors thank the National Science Foundation (CH-0844234) and the Petroleum Research Fund (PRF 49184-ND3) for financial support. We also thank Professor Robert C. Scarrow (Haverford College) for providing us with the original XAS data for CoNHase. The helpful suggestions and insight of the anonymous reviewers was greatly appreciated. XAS data were obtained at the National Synchrotron Light Source (Brookhaven National Laboratories), which is funded by the DOE, Office of Science, Office of Basic Energy Sciences, under Contract No. DE-AC02-98CH10886.

Supporting Information Available: Contains coordinates and additional data for the computational models, electronic absorption spectra comparing NHase-m1, [Co^{II}NHase-m1], and [Co^{III}NHase-m1], the UV−vis-NIR and CD spectra of [Co^{II}NHase-m1], alternate fits to the EXAFS data for [Co^{III}NHase-m1], ^{13}C−NMR data for the catalysis reactions, GPC and mass-spectral data for [Co^{III}NHase-m1] and the CD spectrum of [Co^{III}NHase-m1] following extended air exposure, IR spectrum of [Co^{III}NHase-m1] in H_2O versus D_2O buffer, details for reference 114 and the full author list for reference 79. This material is available free of charge via the Internet at http://pubs.acs.org.

(129) Dey, A.; Jeffrey, S. P.; Darensbourg, M.; Hodgson, K. O.; Hedman, B.; Solomon, E. I. *Inorg. Chem.* **2007**, *46*, 4989–4996.
(130) Yano, T.; Ozawa, T.; Masuda, H. *Chem. Lett.* **2008**, *37*, 672–677.